[Article begins on next page]

Long-term hydroclimate variability in the sub-tropical North Atlantic and anthropogenic impacts on lake ecosystems: A case study from Flores Island, the Azores

Nora Richter[a, b,1]*, James M. Russell[a], Linda Amaral-Zettler[a,b,c,d], Wylie DeGroff[a], Pedro

M. Raposeiro[e,f], Vítor Gonçalves[e,f], Erik J. de Boer[j], Sergi Pla-Rabes[g,h], Armand

Hernández[i], Mario Benavente[j], Catarina Ritter[e], Alberto Sáez[k], Roberto Bao[i], Ricardo

Trigo[l], Ricardo Prego[m], and Santiago Giralt[j]

[a]*Department of Earth, Environmental and Planetary Sciences, Brown University,
Providence, RI 02912, USA*

[b]*The Josephine Bay Paul Center for Comparative Molecular Biology and Evolution,
Marine Biological Laboratory, Woods Hole, MA, 02543, USA*

[c]*Department of Marine Microbiology and Biogeochemistry, NIOZ Royal Netherlands Institute for Sea Research, AB
Den Burg, The Netherlands*

[d]*Department of Freshwater and Marine Ecology, Institute for Biodiversity and Ecosystem Dynamics, University of
Amsterdam, Amsterdam, The Netherlands*

[e]*Centro de Investigação em Biodiversidade e Recursos Genéticos, CIBIO, InBIO Laboratório Associado, Pólo dos
Açores, Portugal*

[f]*Faculdade de Ciências e Tecnologia da Universidade dos Açores, Ponta Delgada, Açores, Portugal*

[g]*CREAF & UAB, Cerdanyola del Vallès, Barcelona, Spain*

[h]*Department of Geography, Environmental Management and Energy Studies, University of Johannesburg, Corner
Ditton and University Avenue, Auckland Park, Johannesburg, South Africa*

[i]*Universidade da Coruña, GRICA Group, Centro de Investigacións Científicas
Avanzadas (CICA), Rúa as Carballeiras, 15071, A Coruña, Spain*

[j]*Geosciences Barcelona (GEO3BCN-CSIC), Spanish National Research Council, Barcelona, Spain*

[k]*UB-Geomodels Research Institute. Department of Earth and Ocean Dynamics, Universitat de Barcelona,
Barcelona, Spain*

[l]*Instituto Dom Luiz (IDL), Faculty of Sciences, University of Lisboa, Lisbon, Portugal*

[m]*Marine Research Institute (IIM), Spanish National Research Council (CSIC), Vigo, Spain*

Corresponding author: Nora Richter
Email: nora.richter@nioz.nl

[1]*Present address*: NIOZ Royal Netherlands Institute for Sea Research, P.O. Box 59, 1790 AB Den Burg, The
Netherlands

Highlights:

- High-resolution paleoclimate and paleoecological reconstruction from Flores Island

- Multi-proxy records distinguish human impacts from climate change

- Early human settlers lowered the resilience of lake ecosystems on remote islands

Abstract

1 **Abstract**

2   Human land use and climate change threaten ecosystems and natural resources,

3 particularly on remote islands such as the Azores Archipelago in the North Atlantic. Since the

4 official Portuguese settlement of the archipelago in the 15th and 16th centuries humans have

5 extensively modified the Azorean landscape, with invasive plants dominating the present-day

6 vegetation and evidence of eutrophication in numerous lakes. To evaluate changes in terrestrial

7 and aquatic ecosystems in the Azores, we developed paleoecological and paleoclimate records

8 from Lake Funda on Flores Island that span the last millennium. Changes in precipitation

9 amount, as recorded by hydrogen isotopes from C_{30} fatty acids (δD_{wax}), suggest that the climate

10 was relatively stable between c. 1000-1400 CE. Recent evidence of early human settlers on the

11 Azorean islands (c. 850-1300 CE) suggests that the introduction of livestock led to an increase in

12 primary productivity in Lake Funda and other lakes in the Azores. More depleted δD_{wax} values

13 between c. 1500-1620 CE suggest that wetter climate conditions existed during the establishment

14 of permanent settlements on Flores Island. Landscape changes between c. 1500-1600 CE

15 coincided with an increase in primary productivity and hypoxic conditions in the lake bottom

16 water, signifying the eutrophication of Lake Funda. Despite reforestation efforts in the Azores in

17 the early 20th century and shift towards drier conditions, eutrophication in Lake Funda persisted.

18 Reforestation efforts likely reduced nutrient leaching and soil erosion in the catchment area of

19 Lake Funda and other Azorean lakes, yet eutrophication continues to be widespread. This

20 highlights the lasting impacts of early human settlers on Lake Funda, and the need for more

21 active remediation efforts.

22

23

24

27
28   **Graphical Abstract:**
29
30

Human activities in the Azores Archipelago & hydroclimate record from Flores Island

First evidence of early human activities on Pico Island

Extensive landscape modification

Drier climate interval on Flores Island

Historical settlement of the Azores Archipelago

Wet climate interval on Flores Island

Variable climate on Flores Island

Trophic state of 23 monitored lakes:
11 eutrophic
10 mesotrophic
2 oligotrophic

Increase in extreme precipitation events in the Azores

Drier climate interval on Flores Island

Year (CE)

Deforestation, increased livestock, & increase in lake trophic state

Increased primary productivity & increase in lake trophic state

Frist evidence of livestock near Lake Funda (coprophilous fungal spores)

Lake Funda remains eutrophic

Reforestation efforts on Flores Island

Major events in Lake Funda, Flores Island

31

1. Introduction

Rising sea levels, changing precipitation patterns, and warmer temperatures threaten island ecosystems that are already under pressure from anthropogenic land use changes (Frias, 2000; Santos et al., 2004; Hoegh-Guldberg et al., 2018). Portuguese settlers shaped the landscape of the Azores Archipelago by replacing dense native laurel forests with exotic plants and agricultural fields, which led to increased soil erosion and left only a few places with native flora and fauna (Dias et al., 2005; Connor et al., 2012; Rull et al., 2017; Raposeiro et al., 2021b). Today the islands are at risk from landslides (Marques et al., 2008), storms and floods (Andrade et al., 2008), and coastal erosion (Calado et al., 2011), and this risk is expected to increase under projected climate change scenarios (Frias, 2000; Santos et al., 2004; Hoegh-Guldberg et al., 2018; Gordo et al., 2019). Although the broad outlines of this history are generally accepted, a more in-depth assessment of past land use changes and climate variability is needed to understand the current state and vulnerability of terrestrial and aquatic ecosystems in the Azores and how past changes in climate influenced human settlement of the islands.

The historically-accepted timing of the settlement of the Azores is close to the onset of the Little Ice Age (LIA, c. 1450-1850 CE), although it is unclear whether this occurred during a wetter or drier climate interval in the subtropical North Atlantic region (Björck et al., 2006; Hernández et al., 2017). Historical records from the 15th century describe the slow establishment and abandonment of early settlements in the central and westernmost islands of the Azores Archipelago due to the isolated location of these islands, infertile land, and/or harsh climate conditions (Smith, 2010). Paleorecords, however, suggest the Azores Archipelago was already inhabited c. 700 years (between c. 700-850 CE) before the arrival of the Portuguese in the 15th century (Raposeiro et al., 2021b). It is unclear whether these settlements persisted until the 15th

55 century, or if they were abandoned before the arrival of the Portuguese. A high-resolution

56 reconstruction of precipitation changes in the Azores and a complementary record of human land

57 use changes could provide insights on how climate change over the last millennium influenced

58 the settlement of the Azores Archipelago, in particular the settlement of Flores Island.

59   The ongoing eutrophication in Azorean lakes is attributed to human activities, including

60 indirect effects such as nutrient loading from the catchment area and direct effects such as fish

61 introductions (Skov et al., 2010; Antunes & Rodrigues, 2011; Cruz et al., 2015; Raposeiro et al.,

62 2017; Vázquez-Loureiro et al., 2019). However, these effects do not explain the high rates of

63 eutrophication observed in lakes isolated from direct human impacts (Antunes & Rodrigues,

64 2011). For instance, Lake Funda on Flores Island is considered to be less impacted by human

65 activities relative to the rest of the Azores Archipelago (Connor et al., 2012), but in the present-

66 day it is considered eutrophic based on high turbidity measurements, as well as nutrient

67 concentrations (i.e., phosphorous) and chlorophyll-α levels (Fig. S1; Cordeiro et al., 2020). It is

68 unclear whether this eutrophication is natural, reflects human modifications in the past, or both.

69 Rising temperatures, changing precipitation patterns, and continued human activities all pose

70 potential risks to these freshwater ecosystems, and threaten their value as a natural resource for

71 the archipelago (Antunes & Rodrigues, 2011).

72   To understand the role of humans and natural climate variability in shaping the present-

73 day landscape, we developed paleoecological and paleoclimate records for Lake Funda on Flores

74 Island. Fecal biomarkers and shifts in vegetation composition indicate when human activities

75 began in the catchment area. In addition, bulk organic and inorganic geochemical proxies, sterol

76 hydrogenation, and archaeal lipids trace changes in organic matter inputs to the lake, redox

77 conditions, and biogeochemical cycles, respectively. Finally, a high-resolution reconstruction

78 using leaf wax hydrogen isotopes records changes in precipitation amount over the last

79 millennium. We investigate the relationships among these variables to determine the interactive

80 effects of climate variations and human activities on Azorean environmental systems.

81

82 **2. Methods**

83 *2.1 Study site*

84 The climate in the Azores is strongly influenced by the Azores anticyclone, leading to

85 increased precipitation from September to March (monthly average precipitation 112 mm) when

86 the storm tracks cross the islands and drier conditions during the late spring and summer months

87 (monthly average precipitation 59 mm) (Santos et al., 2004; Hernández et al. 2016; Global

88 Historical Climatology Network (GHCN)). Maritime conditions result in mild temperatures with

89 mean annual temperatures of 18°C on Flores Island (GHCN).

90 Lake Funda occupies a maar with a 0.37 km^2 surface area, a steep bathymetric gradient,

91 and maximum depth of 35.3 m. The lake is located 351 m a.s.l. at 39°24'N 31°13'W (Figure 1).
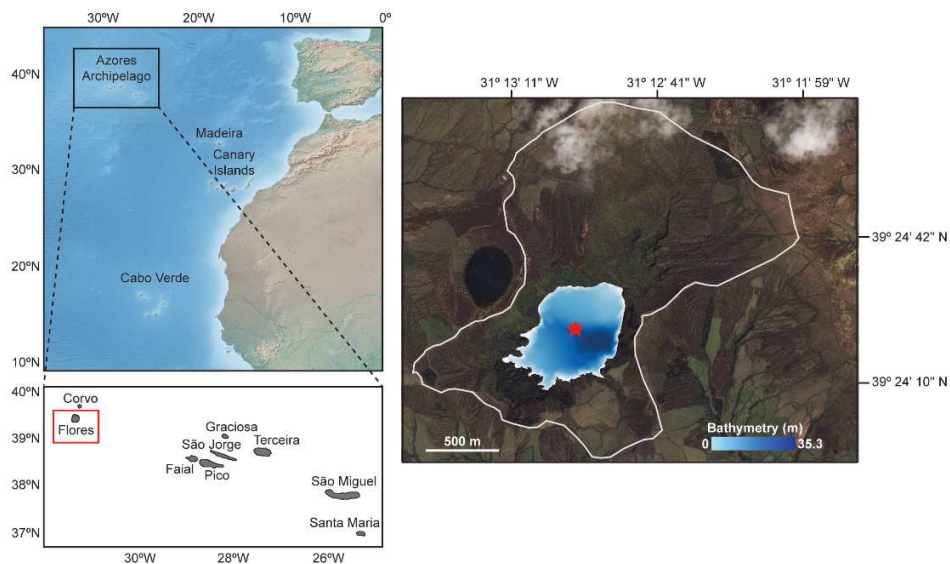
Figure 1. The islands that make up Macaronesia are shown with a close-up of the Azores Archipelago. Lake Funda is located on Flores Island. The bathymetry of Lake Funda is shown and the location of the core analyzed in this study is marked by a red star. The white line outlines the catchment area of Lake Funda. Raster data was obtained from Natural Earth and the maps were rendered in Matlab and ArcGIS.

92   It is located in the interior of Flores Island in the Azores Archipelago and is surrounded by a

93   relatively large (3.14 km^2) and steep catchment area that is mostly forested with some agriculture

94   (Andrade et al., 2019). The lake is monomictic as the lake thermally stratifies from the summer

95   to fall (usually May/June to November) and the water column mixes from November/December

96   to May/June. The lake is considered eutrophic and is usually phosphorus limited (Figure S1).

97   Heightened primary productivity during the spring/summer can lead to rapid oxygen depletion in

98   the water column and hypoxic conditions in the bottom water that leads to internal phosphorus

99   loading (Figure S2).

100

101   *2.3 Sample preparation and analysis*

102   We used a UWITEC® piston corer installed on a UWITEC® platform to retrieve sediment

103   cores from Lake Funda in June 2017 at a water depth of 28.2 m. A total of 9.95 m of sediment

104   were recovered, sealed, and shipped to the Geosciences Barcelona (GEO3BCN-CSIC), where

105   they were kept in a dark room at +4 ºC until they were prepared for analysis. In June 2018, we

106   collected soil samples to differentiate lipids derived from the catchment area from those

107   produced within the lake water column. Soil samples were shipped to the NIOZ Royal

108   Netherlands Institute for Sea Research and were stored at +4 ºC in a dark room until the samples

109   were processed and analyzed for lipids.

110   Cores were split longitudinally and imaged using the high-resolution line scan camera

111   installed on the XRF AVAATECH Core Scanner at the Universitat de Barcelona (UB). Samples

112   were measured for total carbon (TC) and total nitrogen (TN) and the respective isotopic values

113   ($\delta^{13}C$ and $\delta^{15}N$) as described in Raposeiro et al. (2021b). Briefly, samples were analyzed using a

114   ThermoFinnigan Flash- EA1112 elemental analyzer (Thermo Fisher Scientific, Waltham, MA,

115   USA), connected on line to a ThermoFinnigan Deltaplus isotope ratio mass spectrometer

116   (IRMS), at the Servizos de Apoio á Investigación of the Universidade da Coruña (SAI-UDC).

117   Mineralogical analyses were performed with a Bruker D8-A25 diffractometer equipped with a

118   Cu tube (lambda=1.5405 Å) and an ultrafast position sensitive detector (PSD) at the Geo3BCN-

119   CSIC. The carbonate content of these samples was below the detection limit of the X-ray

120   diffractometer, and therefore TC was considered to be equivalent to total organic carbon (TOC).

121   TOC/TN (or C/N) molar ratios were calculated for all measured samples. X-Ray Fluorescence

122   (XRF) was measured on the archived half of the core with the AVAATECH XRF II core scanner

123   at 2 mm intervals. Biogenic silica (BSi) content was determined every 4 cm following Bernárdez

124   et al. (2005) and Mortlock and Froelich (1989), using an Auto Analyzer Technicon AAII at the

125   Marine Research Institute (CSIC) in Vigo.

126   The cores were sampled for lipid analyses, which were processed and analyzed at Brown

127   University and NIOZ. Sediment and soil samples were freeze-dried and lipids were extracted

128   using a Dionex^{TM} accelerated solvent extraction (ASE 350) system with

129   dicholoromethane:methanol (DCM:MeOH, 9:1 v/v) at 120°C and 1200 psi. The resulting

130   extracts were split, with one aliquot processed for glycerol dialkyl glycerol tetraethers (GDGTs)

131   and *n*-alkanes and the other prepared for fatty acid and sterol and stanol analyses.

132   The aliquot for GDGT samples was separated using aluminum oxide (Al_2O_3) columns to

133   obtain a non-polar (hexane (Hex):DCM, 9:1 v/v) fraction containing *n*-alkanes and a polar

134   (DCM:MeOH, 1:1 v/v) fraction for GDGTs. The resulting polar fraction was dried using N_2 gas,

135   and re-dissolved in Hex:Isopropanol (99:1, v/v) and filtered through a 0.4μm PTFE prior to

136   analysis.

137   The acid/polar fraction was separated into neutral (DCM:Isopropanol, 2:1, v/v) and acid

138   (ethyl ether:acetic acid, 24:1, v/v) fractions using an aminopropylsilyl (NH_2) column. The acid

139   fraction was methylated at 60°C for 2 hrs with acidified anhydrous methanol of a known isotopic

140   composition, and the resulting fatty acid methyl ethers (FAMEs) were purified via silica gel (40-

141   63 μm, 60 Å) flash chromatography. The neutral fraction was further separated by silica gel flash

142   chromatography into alkane (Hex), ketone (DCM), and polar (MeOH) fractions. The polar

143   fraction was saponified by dissolving the sample in a 1 M potassium hydroxide solution with

144   MeOH:H_2O (95:5, v/v) and heating it for 3 hrs at 65°C. To this 5% NaCl in H_2O and 50%

145   HCl in H_2O was added, and the lipid fraction was extracted using Hex (100%). The

146   saponified samples were cleaned on a short silica gel column and dried using N_2 gas for

147   derivatization. Pyridine (50 μL) and N,O-Bis(trimethylsilyl)trifluoroacetamide (BSTFA, 50

148   μL) were added to the dried sample, and the sample was capped under N_2 gas and heated for

149   2 hrs at 60°C. The derivatized samples were stored in pyridine until analysis, during which

150   they were dried and re-dissolved in toluene.

151   Samples for GDGTs were analyzed at NIOZ using an Atmospheric Pressure Chemical

152   Ionization/High Performance Liquid Chromatography-Mass Spectrometer (APCI/HPLC-MS)

153   following the method described in Hopmans et al. (2016). An additional 19 samples and

154   replicates were analyzed at Brown University using an APCI/HPLC-MS using the method

155   described in Hopmans et al. (2016). All GDGT results are reported as fractional abundances in

156   this study and concentrations are included for the available samples in the full dataset. The

157   analyses were run using selective ion monitoring to track *m/z* 1302, 1300, 1298, 1296, 1292,

158   1050, 1048, 1046, 1036, 1034, 1032, 1022, 1020, 1018, and 744. This study focuses on

159   isoprenoidal GDGTs (isoGDGTs), but we also quantified and report on branched GDGTs

160   (brGDGTs) in our dataset.

161   All *n*-alkanes and fatty acids were quantified with an Agilent 6890N gas chromatography

162   (GC) system and a flame ionization detector (FID) at Brown University. Samples were injected

163   using pulsed splitless mode (20.3 psi, 310°C) onto a Rtx-200 column (105 m x 205 μm x 0.25

164   μm). The oven program was started at 50°C, ramped up to 315°C at 10°C/min, and then held

165   isothermally for 30 min. All *n*-alkanes were quantified by using hexamethylbenzene as an

166   internal standard.

167   Compound specific isotope ratios (δD_{wax}) of C_{30} FAMES were measured on an Agilent

168   6890 GC equipped with a ZB-1MS (30 m x 320 μm x 0.25 μm) coupled to a Thermo Delta V

169   Plus Isotope Ratio Mass Spectrometer (IRMS) at Brown University. The GC method was run

170   using a pulsed splitless injection mode (30 psi, 320°C), and the oven program was started at

171   40°C for 1 min, and then ramped up to 230°C at 30°C/min where it was held for 1 min. The

172   temperature was increased again to 310°C at 10°C/min and held isothermally for 10 min. The

173   pyrolysis reactor temperature for the IRMS was set at 1450°C. The reference gas $^2H/^1H$ was

174   measured using certified C_{29} and C_{31} *n*-alkane standards. The H^{3+} factor was determined every

175   day, and the mean over the period that samples were measured was 2.41 ± 0.07. An internal

176   standard mixture containing C_{16}, C_{18}, C_{22}, C_{24}, C_{28}, and C_{30} *n*-acids (see Table S1 for analytical

177   uncertainty) was analyzed between every 3 to 4 injections to monitor instrument performance

178   and drift, and a certified C_{30} methyl ester standard of known composition was run to monitor

179   instrument accuracy (lab measured: -186.4 ± 3.9 ‰ for n = 71, actual: -189.4 ± 2 ‰ for n = 5;

180   Schimmelmann, 2018). Each sample was measured three times, and isotopic values were

181   accepted for a voltage response between 2.5 and 7 volts. Isotopic measurements were corrected

182 for the added methyl group, where $\delta D_{MeOH} = -123.7$ ‰ (Tierney et al., 2011). Corrections were

183 made on a daily basis for offsets between measured and reported standard values. All δD_{wax}

184 values are reported relative to the Vienna Standard Mean Ocean Water (VSMOW) in per mil

185 (‰) notation.

186   Sterol and stanol samples were analyzed on an Agilent 7890B gas chromatography

187 (GC) system equipped with an Agilent 5977B quadrupole mass spectrometer (MS) at Brown.

188 Samples were injected using pulsed splitless mode (320°C, 1.3 psi) and run on a ZB-1MS (30 m

189 x 320 μm x 0.25 μm) column. The oven program was started at 40°C for 1 min, and then ramped

190 up to 255°C at 20°C/min and ramped to 315°C at 4°C/min and held isothermally for 10 min. The

191 MS ionization energy was set to 70 eV with a scan range of m/z 50-650. Samples were quantified

192 using select ion monitoring mode and concentrations were determined using 5α-cholestan-3-one

193 as an internal standard (see Table S2).

194

195 *2.2 Age model*

196   We developed the age-depth model (Fig. S3) using ^{210}Pb and ^{137}Cs concentration profiles

197 and ^{14}C dates measured on plant macrofossils in the sediment core (Table S3) as described in

198 Raposeiro et al. (2021b). All radiocarbon dates were calibrated to calendar years (cal yr CE)

199 using the CALIB 7.1 software and the latest INTCAL20 curve (Reimer et al., 2020). In the lower

200 half of the sedimentary sequence (S4), six layers corresponding to gravelly alluvial sediments,

201 rich in terrestrial plant remains that were deposited as single, instantaneous episodic flood

202 events, were removed from the age model. The final age model was developed using the R

203 package clam version 2.3.9 (Blaauw, 2020). The confidence interval of the resulting age-depth

204 model fluctuates between 1 and 50 years throughout the record. In the age-depth model there is a

205 significant increase in the sedimentation rate at 221 cm of core depth which coincides with a

206 lithological change from massive-brown silty clays to centimeter-thick laminated green and

207 yellowish clays. This lithological change was interpreted as deepening in the lake water column

208 (Ritter et al., 2022).

209

210 *2.4 Data processing and breakpoint analysis*

211 Lipid and sediment fluxes were calculated using changes in dry bulk density and

212 sedimentation rates in the sediment core. Potential changes in preservation conditions were

213 assessed by normalizing lipid concentrations to total organic carbon. To determine when

214 significant changes occurred in the sediment record, all datasets were re-sampled first to a 20-yr

215 resolution (except for the sterol and stanol samples) and to a 60-yr resolution to include the sterol

216 and stanol samples. Breakpoint analysis was conducted on the slopes of the re-sampled datasets

217 using the "segmented" package in R version 3.3.3 (R Development Team; Muggeo, 2008).

218 The breakpoints that were common to both re-sampled datasets are reported. The 95%

219 confidence intervals were determined by calculating the pooled uncertainty from the breakpoint

220 analysis and age model.

221

222 *2.5 Leaf waxes as a proxy for vegetation change*

223 Shifts in vegetation were assessed by measuring changes in the *n*-alkane distribution.

224 Higher-level plants produce longer-chain *n*-alkanes (e.g., C_{25}-C_{33}), and can be used to further

225 differentiate grasses and shrubs, which typically produce higher concentrations of C_{31} *n*-alkanes,

226 from woody plants (C_{27} and C_{29}) based on differences in the average chain length (Cranwell,

227   1973; Maffei, 1996). Therefore, shifts in the average chain length (ACL) are often used to

228   reconstruct changes in vegetation as follows:

229

230    $$ACL_{27\text{-}33} = \sum \frac{C_i \times [C_i]}{[C_i]} \qquad [2]$$

231

232   where $[C_i]$ represents the concentration of *n*-alkanes and C_i corresponds to the hydrocarbon

233   chain-length.

234

235   *2.6 Sterols and stanols as fecal biomarkers and indicators of lake water column redox conditions*

236   Sterols and stanols are structurally diverse and relatively stable compounds in the

237   geologic record, making them useful tracers of inputs and microbial activity in the sediment (e.g.

238   Nishimura & Koyama, 1977; Volkman, 1986; Leeming et al., 1996). For instance, C_{29}-sterols are

239   mainly produced by terrestrial plants and certain species of phytoplankton, whereas C_{27}-sterols

240   are derived from cholesterol and are therefore predominantly aquatic in origin (Nishimura &

241   Koyama, 1977; Huang & Meinschein, 1976, 1979; Volkman, 1986). $5\alpha(H)$-stanols, however, are

242   present in low abundance in living organisms and are mainly derived from the microbial

243   reduction of Δ^5-sterols in the sediment (Gaskell & Eglinton, 1975; Nishimura & Koyama, 1977;

244   Rieley et al., 1991). The conversion of Δ^5-sterols to $5\alpha(H)$-stanols is dependent on both the

245   contribution of autochthonous and allochthonous organic matter to the sediment and the redox

246   potential (Nishimura, 1977). The ratio of $5\alpha(H)$-stanols/Δ^5-sterols can thus be used to track

247   changes in inputs and the redox potential, and is calculated as follows:

248

249 $$\frac{5\alpha(H)\text{-stanols}}{\Delta^5\text{-sterols}} = \frac{\text{cholestanol + campestanol + stigmastanol + sitostanol}}{\text{cholesterol + campesterol + stigmasterol + }\beta\text{-sitosterol}} \qquad [3]$$

250

251 An increase in $5\alpha(H)$-stanols/Δ^5-sterols indicates more reducing conditions in the sediment, and

252 also highlights the preferential degradation of Δ^5-sterols relative to $5\alpha(H)$-stanols in the sediment

253 (Gaskell & Eglinton, 1975; Nishimura, 1977; Nishimura & Koyama, 1977).

254   Certain 5β-stanols are produced in high abundance in the gastrointestinal tract of higher

255 mammals, making them biomarkers for fecal inputs from these organisms (Leeming et al., 1996).

256 For instance, carnivores and omnivores, particularly humans, consume large quantities of

257 cholesterol that gets microbially reduced to coprostanol (5β-cholestan-3β-ol) and epi-coprostanol

258 (5β-cholestan-3α-ol) by their gut microbiome (Leeming et al. 1996). Ruminants, on the other

259 hand, reduce a high proportion of plant sterols, e.g. sitosterol and stigmasterol, to 24-

260 ethylcoprostanol and 5β-stigmastanol, respectively (Leeming et al., 1996; Bull et al., 2002). A

261 high abundance of coprostanol, epi-coprostanol, 24-ethylcoprostanol, or 5β-stigmastanol relative

262 to background conditions, could indicate that humans and/or livestock were present in the

263 catchment area of a lake.

264

265 *2.7 Isoprenoidal glycerol dialkyl glycerol tetraethers (isoGDGTs) in lakes*

266   Isoprenoidal glycerol dialkyl glycerol tetraethers (isoGDGTs) are traditionally used as

267 proxies for sea surface temperatures but are also used in lake studies as indicators for specific

268 archaea (e.g. Sinninghe Damsté et al., 2009; Schouten et al., 2013). In particular, changes in lake

269 trophic state and dissolved oxygen content can drive shifts in archaeal communities that produce

270 isoGDGTs, making them useful tracers for paleo-ecological studies (e.g. Blaga et al., 2009;

271 Naeher et al., 2014).

272   Crenarchaeol (Cren) and its regioisomer, Crenarchaeol' (Cren') are specific to

273   *Thaumarchaeota*, or ammonia-oxidizers, in particular groups I.1a and I.1b (Sinninghe Damsté et

274   al., 2002, 2012; Pearson et al., 2004; Schouten et al., 2008; Pitcher et al., 2010, 2011). Group

275   I.1a is found in high abundance near the thermocline and nitrocline in lakes, and is associated

276   with the production of Cren and minor amounts of GDGT-0 and Cren' (Sinninghe Damsté et al.,

277   2002; Auguet et al., 2011, 2012; Pitcher et al., 2011; Buckles et al., 2013). Cren' is produced in

278   higher abundance by *Thaumarchaeota* group I.1b both in soils and in the water column (Pitcher

279   et al., 2010; Sinninghe Damsté et al., 2012; Buckles et al., 2013; Kumar et al., 2019).

280   Identifying different producers of GDGT-0 is more complex, as GDGT-0 can be

281   produced by methanogenic *Euryarchaeota* (Pancost et al., 2000), anaerobic methane-oxidizing

282   Archaea (Pancost et al., 2001; Wakeham et al., 2003), heterotrophic uncultured crenarchaeotal

283   groups (Buckles et al., 2013), and even *Thaumarchaeota* in low abundance (Sinninghe Damsté et

284   al., 2002, 2012; Pitcher et al., 2011). Anaerobic methane-oxidizing archaea can be distinguished

285   by a concurrent increase in the fractional abundance of GDGTs-0, -1, and -2 (Pancost et al 2001;

286   Wakeham et al, 2003), whereas methanogenic *Euryarchaeota* are dominated by GDGT-0 and

287   only minor amounts of GDGT-1 and -2, and no crenarchaeol (Pancost et al., 2000; Blaga et al.,

288   2009; Naeher et al., 2014).

289

290   **3. Results**

291   *3.1 Lacustrine sedimentary units*

292   Prior to c. 1000 CE the core is composed of light brown silty mud that is interspersed

293   with numerous erosive layers of poorly sorted pebbles and sand arranged in fining-upward grain-

294   size sequences that are most likely associated with mass-wasting events (Unit 1, Figure S4).

295   Between c. 1000-1450 CE the core consists of mud interbedded with six thin layers of sand and

296   one layer of gravel-sized clasts c. 1200 CE (Unit 2). The uppermost section of the core is

297   characterized by laminated sediments between c. 1450-2000 CE (Unit 3). The laminations

298   consist of darker lamina composed of silt and clay and lighter layers rich in diatoms. At the very

299   top of the core (c. 2000-2015 CE), there is a shift back to massive brown-black mud (Unit 4).

300

301   *3.2 Hydroclimate variability in the Azores*

302   The distribution of FAMEs in the Lake Funda record is dominated by C_{26} (850-1580 CE)

303   and C_{28} (1581-1940 CE; Figure S5). A high fractional abundance of C_{28} FAMEs was previously

304   reported in a permanently stratified lake in Eastern Africa, and was attributed to the combined

305   input from terrestrial plant material and *in situ* production (van Bree et al., 2018). C_{30} FAMEs,

306   however, are predominantly sourced from terrestrial plants and were therefore targeted for

307   compound-specific hydrogen isotope measurements in this study.

308   In the δD_{wax} record of C_{30} FAMES the variance is low ($\sigma^2 = 6$ ‰) between c. 1000-1400

309   CE (Figure 2). Breakpoints at 1462 ± 14 CE and 1514 ± 13 CE correspond to a change from

310   more enriched to depleted values in δD_{wax} (Table 1). After c. 1400 CE, the variance in the δD_{wax}

311   values increases ($\sigma^2 = 16$ ‰) with periods when δD_{wax} is depleted c. 1500-1620 and 1660-1860

312   CE and a period of enriched δD_{wax} values occurring c. 1880-1980 CE. A sharp depletion from c.

313   1980-1995 CE is followed by enriched δD_{wax} values after c. 2000 and a return to more depleted

314   values c. 2010 CE.
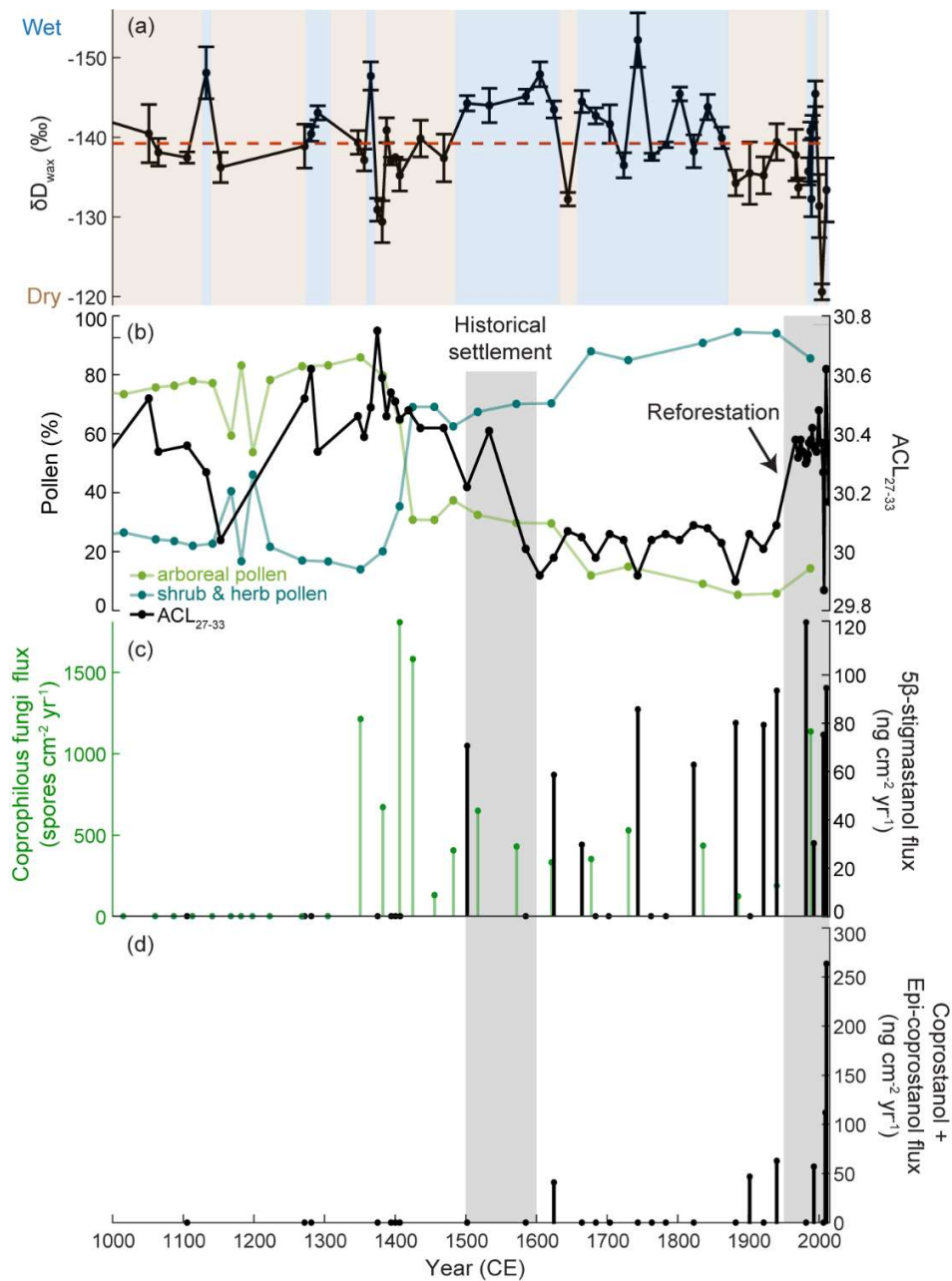
Figure 2. (a) Changes in hydroclimate are noted by shifts in FAMES C_{30} δD_{wax}, where more depleted isotopes correspond to wetter conditions and enriched isotopes correspond to drier conditions (the dashed red line corresponds to the mean of the dataset). Intervals where the climate was wetter or drier are denoted by blue and brown bars, respectively. Major changes in vegetation composition are noted by shifts in **(b)** ACL_{27-33} and are compared with results arboreal (green) and shrub and herb (blue) pollen data (Raposeiro et al., 2021a; Ritter et al., 2022). Fecal biomarkers, including **(c)** coprophilous fungal spores (green) and 5β-stigmastanol (black) and **(d)** coprostanol and epi-coprostanol (Raposeiro et al., 2021a; Ritter et al., 2022), are used to determine when livestock and humans were present in the catchment area. The first gray bar marks the first signs of human activities in the 16th century, and the second gray bar indicates when reforestation efforts started c. 1950 CE.

316   *3.3 Changes in sediment composition and geochemistry*

317   Before c. 1300 CE, C/N values are about 18 but then decrease between 1319 ± 36 CE

318   and 1602 ± 16 CE to about 10 (Figure 3 & Table 1). Biogenic silica (BSi) increases after 1314 ±

319   33 CE and plateaus after 1372 ± 47 CE. This change coincides with an abrupt decrease in $\delta^{15}N$

320   at 1343 ± 37 CE and a further decrease between 1492 ± 11 CE and 1671 ± 8 CE (Figure 3).

321   There is also a gradual decrease in $\delta^{13}C$ values after 1570 ± 14 CE (Figure 4).

322

323   *3.4 Changes in the lake catchment and lake redox conditions*

324   To infer specific changes in the lake catchment, ACL_{27-33} is used to track changes in the

325   vegetation composition and sterols and stanols are used as proxies for the local presence of

326   livestock and humans and as an indicator of changing redox conditions in the lake sediment.

327   Breakpoints for ACL_{27-33} at 1386 ± 39 CE and 1582 ± 12 CE mark a shift towards a decreasing

328   trend in ACL_{27-33} (Figure 2 & Table 1). Unfortunately, we do not have access to native and

329   endemic plants from the Azores to determine the *n*-alkane signatures, so we interpret the

330   decrease in *n*-alkane distribution to reflect a decrease in native gymnosperms based on surveys of

331   alkane distributions in global vegetation (Diefendorf et al., 2011). This interpretation is

332   consistent with palynological data indicating a decrease in *Juniperus brevifolia* (Seub.) Antoine

333   and *Picconia azorica* (Tutin) Knobl and a gradual increase of native grasses (Poaceae) and

334   shrubs (e.g. *Erica azorica* Hochst. ex Seub and *Myrsine*) in the pollen record (Connor et al.,

335   2012; Raposeiro et al., 2021a, b). The flux of sterols and stanols increases between c.1200-1500

336   CE, except for coprostanol, epi-coprostanol, and 5β-stigmastanol (Figure S6). 5β-stigmastanol

337   first occurs c. 1500 CE, but does not become frequent in the sediment record until after c. 1620

338   CE (Figure 2). There is one occurrence of coprostanol c. 1620 CE, however, coprostanol and epi-

339 coprostanol do not become abundant in the sediment record until after c. 1900 CE. An increase

340 in sterols and stanols relative to TOC occurs after c. 1400 CE (Figure S7). This coincides with an

341 increase in $5\alpha(H)$-stanols/Δ^5-sterols after 1481 ± 20 CE and a continued increase in this ratio

342 until the present (Figure 4). ACL_{27-33} values increase again after 1943 ± 9 CE.

343

344 **Table 1.** Segmented breakpoint analysis for the proxy records discussed in this study with the pooled uncertainty
345 shown. The direction of change indicates whether the proxy value increased (+), decreased (-), or did not change (no
346 change).
347

|	Proxy	Segmented Breakpoint Analysis		Direction of Change
		Year (CE)	95% CI (±)	
Climate	δD_{wax} C_{30} FAMES (‰)	1462	14	- (depleted)
		1514	13	+ (enriched)
Catchment area	ACL_{27-33}	1386	39	-
		1582	12	No change
		1943	9	+
Organic matter sources & lake biogeochemical cycles	C/N	1319	36	-
		1602	16	No change
	BSi (%)	1314	33	+
		1372	47	+
	$\delta^{15}N$ (‰)	1343	37	-
		1388	36	+/No change
		1492	11	-
		1671	8	No change
	Cren'/Cren	1352	39	-
		1421	13	+
		1868	12	-
	GDGT-0/Cren	1544	15	+
		1634	15	+
	$\delta^{13}C$ (‰)	1570	14	- (depleted)
Redox conditions	$5\alpha(H)$-stanols/sterols	1481	20	+

348
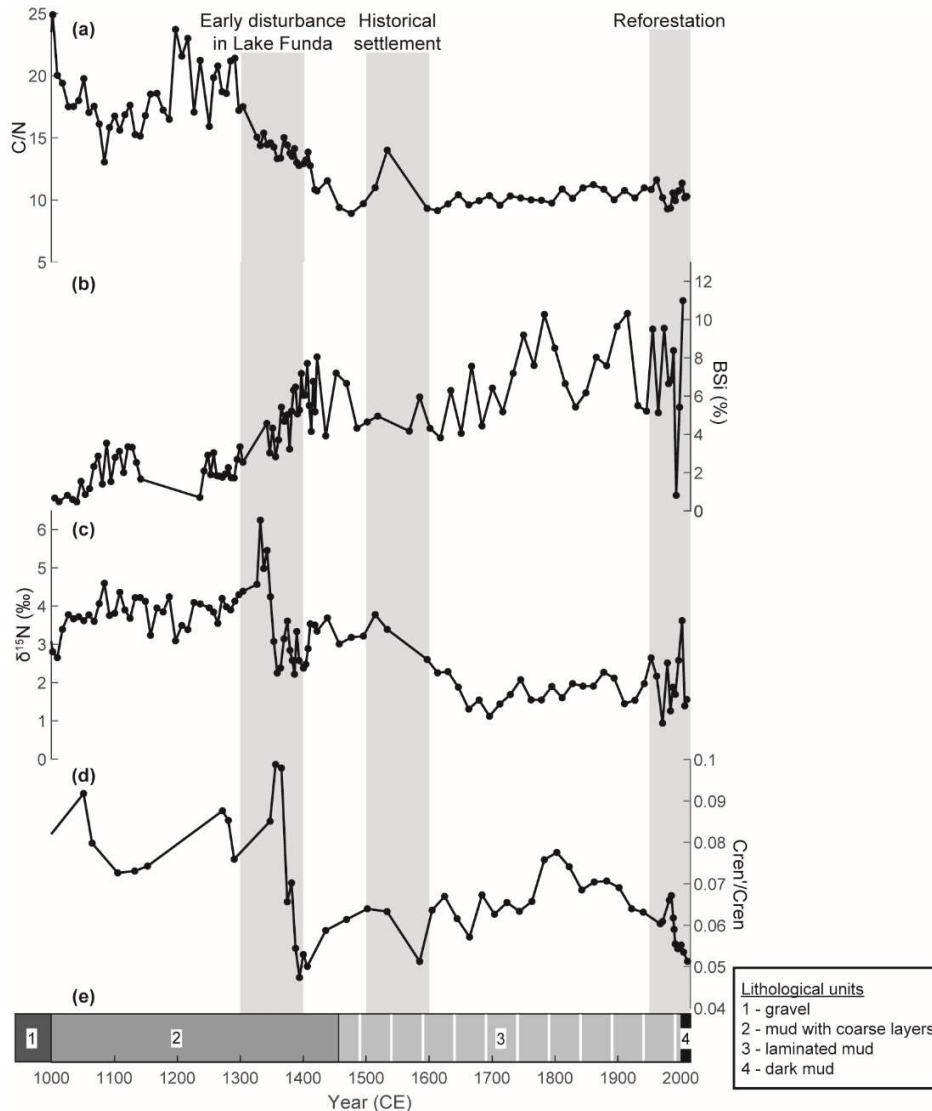
Figure 3. Changes in organic matter inputs to the lake are noted by shifts in **(a)** C/N and are compared with **(b)** changes in diatom productivity, BSi (%). Further changes in the lake are noted by **(c)** $\delta^{15}N$ and **(d)** Cren'/Cren corresponds to changes in the *Thaumarchaeota* community. **(e)** Distinct changes in the sediment core are noted by the different lithological units. The first gray bar indicates coincident changes in the sediment record. The second gray bar corresponds to the historical settlement of Flores Island in the 16th century and the final gray bar corresponds to recent reforestation efforts (c. 1950 CE to the present).

3.3 isoGDGTs as tracers of biogeochemical cycles in the lake water column

In Lake Funda, the composition of isoGDGTs identified in the sediment are distinctly different from the isoGDGT composition of the soils in the catchment, indicating that most of the isoGDGTs in the sediment are produced in the water column (Figure S8). Throughout the

21

361   sediment record GDGT-0 is present in higher abundance relative to other isoGDGTs, and Cren

362   and Cren' are both present throughout the record. Two distinct breakpoints occur in the isoGDGT

363   composition: a decrease in Cren'/Cren between 1352 ± 39 CE and 1421 ± 13 CE and an

364   increase in GDGT-0/Cren about 1544 ± 15 CE (Figure 3 & 4). The later increase in GDGT-0

365   relative to Cren also coincides with a decrease in GDGTs-1 and -2 (Figure S8).

366
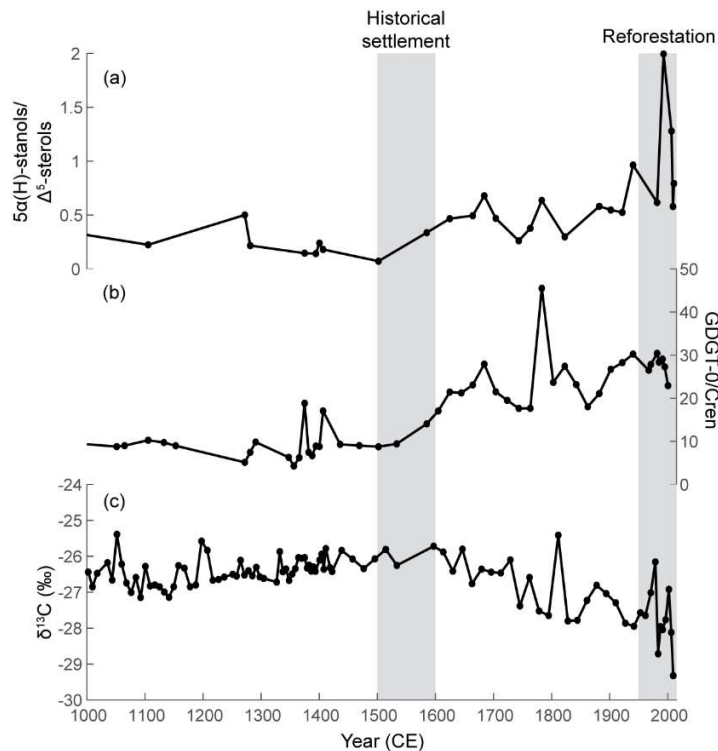
Figure 4. Redox conditions in the lake bottom water are noted by changes in **(a)** 5α(H)-stanols/Δ^5-sterols. Similarly, **(b)** GDGT-0/Cren reflects changes in lake bottom water processes and changes in **(c)** δ^{13}C are shown for comparison. The gray bars correspond to when human activities were first detected in the catchment area in the 16th century and the reforestation efforts that began c. 1950 CE.

4. Discussion

4.1 Controls on leaf wax hydrogen isotopes in the Azores

The hydrogen isotope composition of leaf waxes (δD_{wax}) in higher terrestrial plants (i.e. C_{28}-C_{32} *n*-acids) is correlated with changes in δD of precipitation (δD_{precip}; Sachse et al., 2012). The variability in δD_{precip} reflects a combination of processes, including precipitation amount, water source, transport history, and Rayleigh-type processes related to evaporation and condensation (Craig, 1961; Dansgaard, 1964; Sachse et al., 2012). In the Azores changes in precipitation amount, and also δD_{precip}, are dominated by shifts in the high-pressure Azores anticyclone, resulting in both intra- and interannual variability associated with the North Atlantic Oscillation (NAO; Hurrell, 1995; Santos et al., 2004; Cropper & Hanna, 2014; Hernández et al., 2016). In the Azores, mean monthly event-based δD_{precip} from 1963-2014 is negatively correlated with precipitation amount during the drier spring (MAM, r = -0.72, p<0.01) and summer (JJA, r = -0.49, p<0.05) months and wetter fall (SON, r = -0.41, p<0.05) season (Table 2; Global Network of Isotopes in Precipitation (GNIP); Rubio de Inglés, 2016). The majority of vapor mass originates from the tropical and sub-tropical regions of the Atlantic (including the Gulf of Mexico), however, the vapor mass that reaches the Azores Archipelago receives additional vapor inputs over the North Atlantic Ocean such that the isotopic variability associated with source changes does not have a major impact on δD_{precip} (Araguás-Araguás et al., 2000; Gimeno et al., 2010; Rubio de Inglés, 2016). In addition, a temperate oceanic climate leads to small variations in air temperature on Flores, with average temperatures ranging from 15°C during the winter months (DJF) to 23°C during the summer (JJA), and has a minimal influence on δD_{precip} (Dansgaard, 1964; Baldini et al., 2008; Rubio de Inglés, 2016; Global Historical Climatology

389 Network (GHCN)). Therefore, we infer that the δD_{wax} of higher terrestrial plants is primarily

390 influenced by changes in precipitation amount.

391
392 **Table 2.** Spearman rank correlation coefficients comparing mean monthly air temperature and precipitation amounts
393 with event-based δD_{precip}. The instrumental data is obtained from Ponta Delgada (1963-2014; Hernández et al., 2016;
394 Global Network of Isotopes in Precipitation (GNIP)).
395

	Air Temperature vs. δD_{precip}		Precipitation amount vs. δD_{precip}	
	r	**p**	**r**	**p**
Winter (DJF)	-0.09	0.63	-0.35	0.07
Spring (MAM)	0.30	0.14	**-0.72**	**<0.01**
Summer (JJA)	-0.07	0.74	**-0.49**	**<0.05**
Fall (SON)	0.13	0.51	**-0.41**	**<0.05**

396

397

398 *4.2 Impacts of early human activities on Lake Funda (c. 1000-1400 CE)*

399   The Portuguese are thought to have discovered and settled the Azores in the 15th century

400 (Crosby, 2004). However, the Canary Islands, and possibly the Azores and Madeira, were

401 already known to the Romans (c. 500 BCE) and Isidor de Sevilla (c. 600 CE), and in the 14th

402 century the Azores Archipelago was included on maps and in atlases (Schäfer, 2003; Crosby,

403 2004; see Raposeiro et al., 2021b). Paleoecological records from two Azorean islands (Corvo

404 and Pico), show an almost simultaneous increase of fire-related proxies (e.g. charcoal particles

405 and polycyclic aromatic hydrocarbons) and fecal biomarkers (e.g. 5β-stigmastanol and

406 coprophilous fungal spores) suggesting that humans first arrived in the archipelago between c.

407 700-850 CE (Raposeiro et al., 2021b). Thus, it is likely that, at the very least, limited or

408 temporary settlements existed well before the 15th century.

409   Between c. 1000-1500 CE there are very few changes in the ACL_{27-33} record, and pollen

410 data indicates that dense laurel forests dominated the catchment of Lake Funda (Connor et al.,

411 2012; Raposeiro et al., 2021b). In addition, the δD_{wax} record from Lake Funda is characterized by

412 low variability and relative D-enrichment between c. 1000-1400 CE, suggesting that the climate

413 was relatively dry and stable (Figure 2). This coincides with overall drier conditions in Morocco

414 (c. 1000-1400 CE; Esper et al., 2007; Wassenburg et al., 2013; Ait Brahim et al., 2017) and the

415 Iberian Peninsula (c. 900-1300 CE; Sánchez-López et al., 2016). Similarly, results from the

416 Community Earth System Model (CESM-CAM5_CN) Last Millennium Ensemble transient

417 simulation suggest that early settlers encountered overall drier and warmer climate conditions

418 between c. 800 CE and the onset of the Little Ice Age (c. 1350-1450 CE; Raposeiro et al.,

419 2021b).

420   A decrease in C/N values and an increase in BSi after c. 1300^{+32}_{-28} CE corresponds to a

421 transition from terrestrially dominated to aquatically sourced organic matter inputs and

422 heightened productivity (Figure 3; Raposeiro et al., 2021b). A decrease in Cren'/Cren (Figure 4)

423 could also be a result of heightened primary productivity as ammonium concentrations increase

424 in the water column from the decomposition of particulate organic matter (Blaga et al., 2011;

425 Auguet et al., 2011, 2012; Kumar et al., 2019). This could promote increased ammonia oxidation

426 by *Thaumarchaeota* Group I.1a at the oxycline/thermocline and nitrocline, resulting in increased

427 Cren production relative to Cren' (Sinnighe Damste et al., 2009; Auguet et al., 2011, 2012; Blaga

428 et al., 2011; Kumar et al., 2019). The depletion in $\delta^{15}N$ at c. 1350^{+44}_{-34} CE differs from the

429 expected enrichment of $\delta^{15}N$ that is usually associated with increased primary productivity and a

430 decrease of terrestrial material (Hodell & Schelske, 1998; Brenner et al., 1999; Meyers et al.,

431 2003). The depletion in $\delta^{15}N$ occurs shortly after the first appearance of coprophilous fungal

432 spores (i.e., *Sporormiella, Sordaria,* and *Podospora*) c. 1350^{+44}_{-34} CE. We infer that the depletion

433 in $\delta^{15}N$ reflects an increase in N-fixation, which could result from the presence of livestock in the

434 catchment area that led to an increase of phosphorous inputs to Lake Funda (Raposeiro et al.,

435 2021b). Many lakes in the Azores, including Lake Funda, are phosphorus limited and increased

436 phosphorus inputs to the lake from livestock could lead to increased N_2-fixation by

437 cyanobacteria, lower $\delta^{15}N$ values, and promote eutrophication (Brenner et al., 1999; Meyers,

438 2003; Cruz et al., 2015; Raposeiro et al., 2021b).

439   The lack of 5β-stigmastanol in our record despite the increase in fungal spores at this

440 time could reflect differences in the preservation, transport, or deposition of fungal spores

441 relative to fecal stanols (Guillemont et al., 2017; Zocatelli et al., 2017). Fungal spores are local

442 indicators of megaherbivores that can be transported via run-off or wind across 25-100 m (Gill et

443 al., 2013; Perrotti & van Asperen, 2019), and further transported on and within the lake. The

444 water-solubility of 5β-stanols is low and they are typically bond to clays and particulate organic

445 matter, so their input to lake sediments is limited to run-off and riverine inflows (Walker et al.,

446 1982; Lloyd et al., 2012). In the case of Lake Funda, the steep catchment makes the lake difficult

447 to access, so humans and/or livestock likely only sought out the lake during drier climate

448 conditions, e.g. between c. 1300-1350 CE and c. 1370-1390 CE, and that the influx of 5β-stanols

449 to the lake is likely reduced relative to fungal spores. For comparison, Lake Caldeirão is shallow

450 lake on Corvo Island is located in a wide crater with gentle slopes, making the lake easily

451 accessible to humans and livestock. In the present-day, livestock can be found at the edge of the

452 lake year-round. A higher concentration of both fecal stanol and coprophilous fungal spores

453 likely reach the lake sediment via run-off, which would explain the similar trends observed in the

454 fecal stanol and coprophilous fungal spore records from c. 700-850 CE to the present (see

455 Raposeiro et al., 2021b). In contrast, Lake Peixinho on Pico Island (870 m a.s.l) is more exposed

456 to the elements and is located at a higher altitude than Lake Funda (351 m a.s.l.) and Caldeirão

457 (410 m a.s.l.), such that fungal growth is likely limited by colder temperatures or the fecal

458   material is washed away before the fungus has enough time to germinate (Dickinson &

459   Underhay, 1977; Wood & Wilmshurst, 2012; Perrotti & van Asperen, 2019). In this case, we

460   might observe a higher influx of 5β-stanols relative to fungal spores, which might explain the

461   early appearance of 5β-stanols (c. 700-850 CE) and the lack of fungal spores until c. 1100 CE in

462   Lake Peixinho (see Raposeiro et al., 2021b).

463   The increase in nutrient inputs to Lake Funda occurred during stable and drier conditions,

464   as indicated by the low variance and enriched values of δD_{wax}, on Flores Island and without

465   changes in the catchment or noticeable changes in the sediment core. Although there are no

466   significant changes in vegetation composition nor evidence of changes in soil erosion, the

467   introduction of livestock could enhance nutrient cycling in the landscape and result in more open

468   patches of vegetation leading to increased nutrient leaching from soils into the lake from the

469   catchment (e.g. McNaughton et al., 1997). This is also observed in other islands of the Azores

470   Archipelago as well as the Faroe Islands and Iceland, where the introduction of livestock resulted

471   in increased nutrient loading and changes in lake trophic state before noticeable changes in soil

472   erosion and vegetation composition occurred (Hannon et al., 2005; Lawson et al., 2007;

473   Raposeiro et al., 2021b).

474   If early settlements were present on Flores Island, then they were likely abandoned before

475   the 15th century as there are no records of humans living on the island when the first Portuguese

476   explorers and later Flemish and Portuguese settlers arrived in the mid-15th and early 16th century

477   (Raposeiro et al., 2021b). However, the continued decrease in C/N values until c. 1500 CE

478   suggests that Lake Funda was still adjusting to the initial disturbance. Thus, the initial increase in

479   primary productivity in Lake Funda could be evidence of human impacts on the island prior to

480   the accepted settlement of Flores Island and likely made the lake ecosystem more susceptible to

481   later disturbances in the lake catchment.

482

483   *4.2 Environmental impacts of human settlements on Flores Island (c. 1401-1900 CE)*

484   The start of organized Portuguese explorations along the western coast of Africa began in

485   the late 14th to early 15th century (Meneses, 2009) during a drier (enriched δD_{wax} values in the

486   Funda record) climate interval on the Flores Island. Similarly, relatively low lake levels recorded

487   on Pico Island and São Miguel suggest that the climate was overall drier in the Azores

488   Archipelago during the 15th century (Björck et al., 2006; Hernández et al., 2017). After 1432 CE

489   the Portuguese established settlements in Santa Maria and São Miguel, and eventually Flemish

490   settlements were established on Flores Island in 1472 CE but were abandoned after a few years

491   (Schäfer, 2003; Connor et al., 2012; Rull et al., 2017; Raposeiro et al., 2021b). More extensive

492   settlement of Flores Island by the Portuguese began c. 1510 CE during a wetter climate interval

493   recorded by more depleted δD_{wax} values in the Lake Funda record (Lages, 2000; Schäfer, 2003;

494   Connor et al., 2012). Lake-levels in waterbodies on São Miguel, however, continue to decrease

495   after c. 1500 CE (Hernández et al., 2017) and more frequent negative phases in the NAO during

496   the winter season suggest that drier conditions prevailed (Raposeiro et al., 2021b). In this

497   context, the more depleted δD_{wax} values, reflecting wetter conditions, observed in Lake Funda

498   could be attributed to differences in precipitation seasonality. The δD_{wax} record from Flores

499   Island primarily reflects spring and summer precipitation during the period of leaf wax

500   production (Tipple et al., 2012), when we observe the strongest correlation between δD_{precip} and

501   rainfall amount (see Table 2). In contrast, changes in lake-level reflect mean annual changes in

502 precipitation and the NAO is primarily responsible for the variability in winter precipitation

503 (Hernández et al.2016).

504 Despite the relatively recent settlement of the islands, the present-day landscape has been

505 completely altered and it is uncertain how vulnerable this has made the current island ecosystems

506 to climate change (e.g. Antunes & Rodrigues, 2011; Connor et al., 2012; Cruz et al., 2015; Rull

507 et al., 2017). The more frequent occurrence of 5β-stigmastanol after c. 1620 CE in the Lake

508 Funda record likely reflects the widespread release of livestock on the islands to provide food for

509 settlers (Figure 2; Schäfer, 2003; Smith, 2010). This was a common practice among the

510 Portuguese as they settled Macaronesia, for instance, in Cabo Verde the timing of human

511 settlement (c. 1450-1600 CE) coincides with an abrupt increase in non-obligate coprophilous

512 fungi from livestock feces, followed by the gradual proliferation of newly introduced flora and

513 increased erosion (c. 1600-1700 CE; Castilla-Beltrán et al., 2019). Most settlements on Flores

514 were established in low coastal areas (Raposeiro et al., 2021b), which could explain the lack of

515 coprostanol and epi-coprostanol in the lake sediments until the 20th century during a prolonged

516 dry interval as indicated by more enriched δD_{wax} values. On Flores Island, the introduction of

517 livestock coincides with a decrease in ACL_{27-33} between c. 1500-1600 CE, as native vegetation

518 (i.e., *Juniperus brevifolia* and *Picconia azorica*) was cleared to create a more open landscape for

519 livestock (Connor et al., 2012; Raposeiro et al., 2021b). Similarly, in the Canary Islands, early

520 European settlers cleared forests in the lowlands for agriculture and pastures for livestock (de

521 Nascimento et al., 2009). The decrease in ACL_{27-33} that is associated with deforestation on Flores

522 Island is in direct contrast to the increase in ACL_{25-31} that is observed on Iceland as Norse settlers

523 cleared birch trees (Richter et al., 2021). Higher ACL_{27-33} values in Flores could be associated

524 with increased production of longer chain *n*-alkanes by plant species in the family *Juniperus*

525   (C_{33}-C_{35}; Diefendorf et al., 2011), whereas birch trees (*Betula pubescens* and *Betula nana*) in

526   Iceland predominantly produce shorter chain *n*-alkanes (C_{25}-C_{27}; Schwark et al, 2002; Balascio

527   et al. 2018).

528   The effects of Portuguese activities on Lake Funda are apparent beginning about c.

529   1500^{+10}_{-11} CE when laminations rich in diatoms are visible in the sediment record, suggesting that

530   increased nutrient availability led to heightened primary productivity and a further decrease in

531     $\delta^{15}N$ (Figure 3). At this time, however, we also observe a shift to more reducing conditions in the

532   sediment, i.e. an increase in $5\alpha(H)$-stanols/Δ^5-sterols, c. 1500-1550 CE from oxygen depletion in

533   the water column (Figure 4; Gaskell & Eglinton 1975; Nishimura, 1977; Nishimura & Koyama,

534   1977; Kalff, 2002). In addition, increases in GDGT-0/Cren and a decrease in GDGT-1 and -2

535   suggest the production of isoGDGTs by methanogenic archaea in the bottom water of the lake

536   (Figure S7; Pancost et al., 2000; Blaga et al., 2009; Naeher et al., 2014). This is supported by the

537   gradual decrease in bulk $\delta^{13}C$ values after c. 1570 CE as more depleted carbon is added to the

538   epilimnion from increased methanogenesis (e.g. Hollander & Smith, 2001).

539   Increased primary production and evidence of hypoxic conditions in the lake bottom

540   water suggest that Lake Funda underwent a relatively rapid period of nutrient addition, loss of

541   bottom-water oxygen, and thus eutrophication that occurred as land clearance became

542   widespread in c. 1500 CE. In contrast, Lake Azul on São Miguel responded more gradually to

543   human impacts in the catchment area with the lake remaining relatively pristine and oligotrophic

544   until the introduction of exotic fish in the 1800s (Figure 5; Raposeiro et al., 2017). A rapid

545   response in lacustrine ecosystems to human activities is observed during the settlement of

546   Iceland and the Faroe Islands, but less so in Greenland (Hannon et al., 2005; Lawson et al., 2005,

547   2007; Massa et al., 2012; Richter et al., 2021). Cultural eutrophication in Lake Funda after c.

548   1500 CE could reflect a loss of resilience as the lake ecosystem reached a tipping point from

549   repeated disturbances in the catchment (i.e., human activities in c. 1300 CE and c. 1500 CE)

550   and/or an intensification of human activities after c. 1500 CE (Ritter et al., 2022). Such a tipping

551   point could be driven by increased nutrient availability that trigger positive feedbacks between

552   eutrophication, bottom water oxygenation, and internal loading of P (Scheffer, 1998; Marsden,

553   1989). We infer that historic and continued nutrient inputs from the landscape and potential

554   internal phosphorous-loading due to hypolimnetic deoxygenation during the summer months led

555   to an alternative stable state in Lake Funda (Scheffer et al., 2001). A similar loss of resilience

556   from early human activities is observed in lakes in Canada, Greenland, and Switzerland, where

557   even after the settlements were abandoned the lakes remained eutrophic or, if they did recover,

558   were more susceptible to later disturbances (Douglas et al., 2004; Ekdahl et al., 2004; Hillbrand

559   et al., 2014).

560   Despite a shift to more variable and wetter conditions between c. 1660-1860 CE,

561   indicated by more depleted δD_{wax} values, the vegetation composition (ACL_{27-33}) stabilized

562   between c. 1600-1950 CE in the catchment area of Funda (Figure 2). However, $5\alpha(H)$-

563   stanols/Δ^5-sterols and GDGT-0/Cren values continued to increase during this time period, which

564   would suggest that eutrophic conditions in Lake Funda were sustained by hysteresis in the

565   system.

566
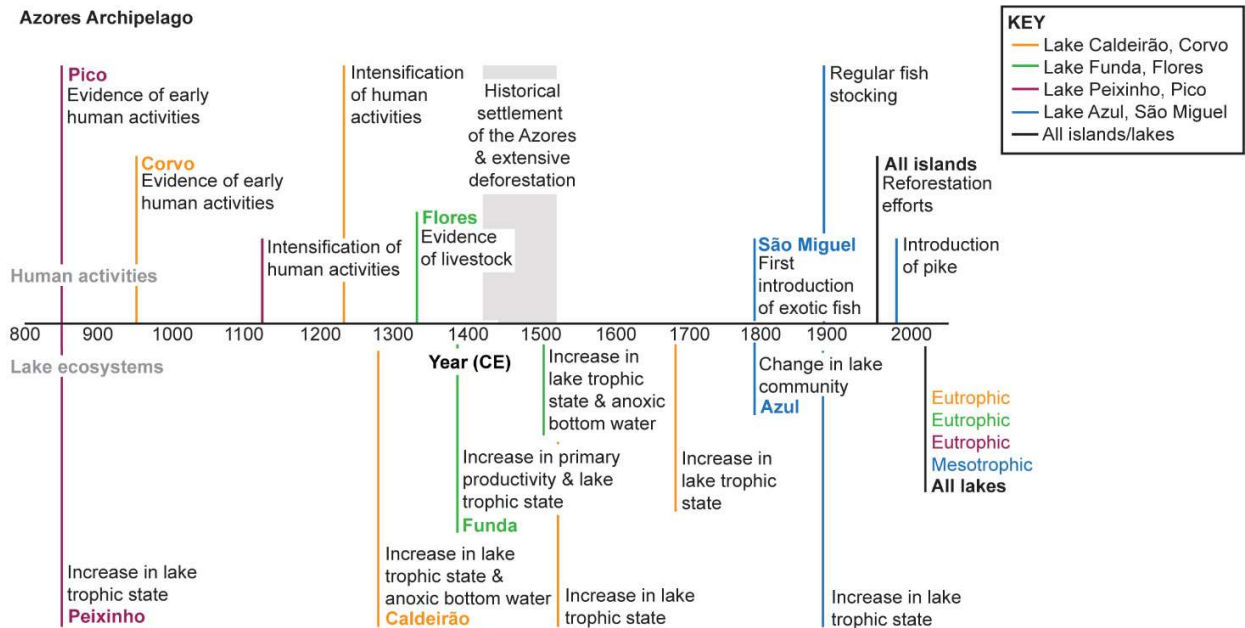
Figure 5. A timeline highlighting major human activities on four different Azorean islands and ecological changes
that occurred in four different lakes on these islands (figure based on data from Raposeiro et al., 2017, 2021b).

567
568

569

4.3 Ecological changes in the Azores in the 20th and 21st centuries (c. 1901-2015 CE)

570

571 The transition from the 19th to early 20th century was marked by major environmental and

572 climatic changes in broader Macaronesia. In Flores, δD_{wax} values remain enriched relative to the

573 mean from c. 1880-1980 CE with a slight depletion from c. 1940-1970 CE followed by a sharper

574 depletion between c. 1980-1995 CE, indicating an overall drier climate until c. 1940 CE

575 followed by a gradual increase in precipitation that peaks c.1980-1995 CE. This is reflected by

576 the gradual increase in precipitation between 1943-2012 recorded in instrumental data from

577 Ponta Delgada, São Miguel (Hernández et al., 2016). However, we do observe a return to drier

578 conditions near the beginning of the 21st century, which could reflect several anomalous years

579 with drier conditions on both Flores Island and São Miguel from 1999-2000 CE and 2003-2005

580 CE before a return to wetter conditions between 2006-2015 CE (Hernández et al., 2016; Global

581 Historical Climatology Network (GHCN)).

582   A sharp increase in ACL_{27-33} values c. 1950 CE in Lake Funda (Figure 2) marks the start

583   of major reforestation efforts, as the local Forestry Service began to actively plant *Cryptomeria*

584   *japonica* in the Azores (Rull et al., 2017; Borges et al., 2019). Similarly, in Cabo Verde exotic

585   trees, such as *Pinus* and *Acacia*, were introduced in the early 20th century to help reduce land

586   degradation (Castilla-Beltrán et al., 2019). The combination of a drier climate and more trees in

587   the lake catchment area in the early 20th century should act to stabilize the soil, which in theory

588   should lead to reduced erosion and external nutrient loading and therefore lower primary

589   productivity and improve oxygenation in the water column. In Lake Funda the lack of changes in

590    $5\alpha(H)$-stanols/Δ^5-sterols and GDGT-0/Cren suggest that there was little change in the microbial

591   community response to changes in erosion and nutrient loading (Figure 4). Limnological surveys

592   over the last two decades confirm that eutrophication continues to be a problem for Lake Funda

593   and hypoxic, and sometimes fully anoxic, conditions develop in the lake bottom water during the

594   summer and fall months (Figure S1 & S2). Continued internal loading of phosphorus and other

595   changes in the nitrogen and carbon cycle could promote the increase in microbially mediated

596   hydrogenation of Δ^5-sterols to $5\alpha(H)$-stanols and methanogenesis in the bottom water that we

597   observe in Lake Funda (Gaskell & Eglinton 1975; Nishimura, 1977; Nishimura & Koyama,

598   1977; Kalff, 2002).

599   Eutrophication is a problem for numerous lakes in the Azores Archipelago, and as

600   exemplified by this case study in Lake Funda and several other paleoecological studies in the

601   Azores, these changes in trophic state can be attributed to past human land use changes and/or

602   the introduction of fish (Figure 5; Skov et al., 2010; Antunes & Rodrigues, 2011; Cruz et al.,

603   2015; Raposeiro et al., 2017). Although external nutrient loads were reduced in Lake Furnas and

604   Sete Cidades (Lake Azul and Lake Verde) on São Miguel, nitrate and phosphorus concentrations

605 in the lakes remain high from N_2-fixation and internal P-loading during the summer months,

606 respectively (Cruz et al., 2015). Lake Funda is faced with a similar scenario, where

607 eutrophication is sustained from internal loading and suggests that more aggressive remediation

608 strategies are needed for the lake ecosystem to recover (Schindler, 2006). In contrast to some of

609 the lacustrine ecosystems in the high North Atlantic (e.g. Iceland, Faroe Islands, and Greenland),

610 Lake Funda underwent what appears to be a permanent shift in trophic state in response to

611 human activities in the landscape (Lawson et al., 2005, 2007; Massa et al., 2012; Richter et al.,

612 2021). Even though settlements were never established in the catchment of Lake Funda, early

613 human activities likely made the lake more susceptible to later disturbances. Our study highlights

614 the importance of understanding early human impacts and the natural state of lake ecosystems, as

615 this can have a large influence on the current trophic state of lakes and the remediation strategies

616 needed to tackle the problem.

617

618 **5. Conclusions**

619 Prior c. 1400 CE, climate on Flores Island was characterized by overall drier and more

620 stable conditions. During the 14th century, increases in primary productivity within Lake Funda

621 indicate a response to heightened nutrient loading from the catchment in response to the earlier

622 arrival of humans on Flores Island. The documented settlement of the Azores Archipelago during

623 the 15th to 16th centuries occurred at the start of the LIA during a prolonged wet period in Flores

624 Island. Increased precipitation most likely contributed to earlier abandonments of settlements on

625 Flores Island between 1452-1510 CE before the establishment of permanent settlements after c.

626 1510 CE (Lages et al., 2009). Increases in 5β-stigmastanol and a rapid decrease in ACL_{27-33} in

627 the 16th century, point to the widespread introduction of cattle and clearance of native vegetation,

628 respectively, on Flores Island by the Portuguese. Increased nutrient inputs to Lake Funda

629 resulted in a permanent shift in the lake trophic state as marked by a further increase in primary

630 productivity and the onset of hypoxic conditions in the lake bottom water. Despite recent

631 reforestation efforts to reduce soil erosion, Lake Funda has remained eutrophic either from

632 sustained nutrient inputs or internal loading of phosphorus. Many of the environmental issues in

633 the Azores are likely to be exacerbated by a warming climate and changes in precipitation. For

634 instance, warming temperatures can lead to prolonged lake stratification that could further

635 exacerbate already eutrophic systems (Woolway & Merchant, 2019). Environmental

636 management strategies need to account for the potential impacts this might have on already

637 vulnerable lake ecosystems.

638

639 **Data Availability**

640 The age model for this core, the total carbon and nitrogen data, the bulk carbon and nitrogen

641 isotopes, the sterol and stanol abundances, and biogenic silica data are available at Raposeiro et

642 al. (2021a; https://doi.pangaea.de/10.1594/PANGAEA.933712). Additional data published in

643 this manuscript are available at Richter et al. (2022; https://doi.org/10.1594/PANGAEA.941316).

644

655

References

657 Ait Brahim, Y., Cheng, H., Sifeddine, A., Wassenburg, J.A., Cruz, F.W., Khodri, M., Sha, L.,

658   Pérez-Zanón, N., Beraaouz, E.H., Apaéstegui, J., Guyot, J.L., 2017. Speleothem records

659   decadal to multidecadal hydroclimate variations in southwestern Morocco during the last

660   millennium. Earth Planet. Sci. Lett., 476, 1-10. https://doi.org/10.1016/j.epsl.2017.07.045

661 Andrade, C., Cruz, J. V., Viveiros, F., Coutinho, R. 2019. CO_2 flux from volcanic lakes in the

662   western group of the Azores Archipelago (Portugal). Water, 11(3), 599.

663   https://doi.org/10.3390/w11030599

664 Andrade, C., Trigo R.M., Freitas, M.C., Gallego M.C., Borges, P., Ramos, A.M., 2008.

665   Comparing historic records of storm frequency and the North Atlantic Oscillation (NAO)

666   chronology for the Azores region. Holocene, 18, 745-754.

667   https://doi.org/10.1177/0959683608091794

668 Antunes, P., Rodrigues, F. C., 2011. Azores Volcanic Lakes: factors affecting water

669   quality. *Water Quality: Currents Trends and Expected Climate Change Impacts*, 106-114.

670 Araguás-Araguás, L., Froehlich, K., & Rozanski, K., 2000. Deuterium and oxygen-18 isotope

671   composition of precipitation and atmospheric moisture. Hydrol. Process., 14(8), 1341-1355.

672   https://doi.org/10.1002/1099-1085(20000615)14:8<1341::AID-HYP983>3.0.CO;2-Z

673 Auguet, J. C., Nomokonova, N., Camarero, L., Casamayor, E. O., 2011. Seasonal changes of

674   freshwater ammonia-oxidizing archaeal assemblages and nitrogen species in oligotrophic

675   alpine lakes. Appl. Environ. Microbiol., 77(6), 1937-1945.

676   https://doi.org/10.1128/AEM.01213-10

677 Auguet, J. C., Triado-Margarit, X., Nomokonova, N., Camarero, L., & Casamayor, E. O. (2012).

678   Vertical segregation and phylogenetic characterization of ammonia-oxidizing Archaea in a

679   deep oligotrophic lake. ISME J., 6(9), 1786-1797. https://doi.org/10.1038/ismej.2012.33

680 Balascio, N. L., D'Andrea, W. J., Anderson, R. S., Wickler, S., 2018. Influence of vegetation

681   type on n-alkane composition and hydrogen isotope values from a high latitude ombrotrophic

682   bog. Org. Geochem., 121, 48-57. https://doi.org/10.1016/j.orggeochem.2018.03.008

683 Baldini, L. M., McDermott, F., Foley, A. M., Baldini, J. U., 2008. Spatial variability in the

684   European winter precipitation δ^{18}O-NAO relationship: Implications for reconstructing NAO-

685   mode climate variability in the Holocene. Geophys. Res. Lett., 35(4).

686   https://doi.org/10.1029/2007GL032027

687 Bernárdez, P., Prego, R., Francés, G., González-Álvarez, R., 2005. Opal content in the Ría de

688   Vigo and Galician continental shelf: biogenic silica in the muddy fraction as an accurate

689   paleoproductivity proxy. Cont. Shelf Res., 25(10), 1249-1264.

690   https://doi.org/10.1016/j.csr.2004.12.009

691 Blaga, C. I., Reichart, G. J., Heiri, O., Damsté, J. S. S., 2009. Tetraether membrane lipid

692   distributions in water-column particulate matter and sediments: a study of 47 European lakes

693   along a north–south transect. J. Paleolimnol., 41(3), 523-540. https://doi.org/10.1007/s10933-

694   008-9242-2

695   Blaga, C. I., Reichart, G. J., Vissers, E. W., Lotter, A. F., Anselmetti, F. S., Damsté, J. S. S.,

696   2011. Seasonal changes in glycerol dialkyl glycerol tetraether concentrations and fluxes in a

697   perialpine lake: Implications for the use of the TEX$_{86}$ and BIT proxies. Geochim.

698   Cosmochim. Acta, 75(21), 6416-6428. https://doi.org/10.1016/j.gca.2011.08.016

699   Blaauw, M., Christen, J. A., Vazquez, J. E., Goring, S., Clam - Classical Age-Depth

700   Modelling of Cores from Deposits. R Packag. Version 2.3.9 (2020)

701   Björck, S., Rittenour, T., Rosén, P., França, Z., Möller, P., Snowball, I., Wastegård, S., Bennike,

702   O., Kromer, B., 2006. A Holocene lacustrine record in the central North Atlantic: proxies for

703   volcanic activity, short-term NAO mode variability, and long-term precipitation

704   changes. Quat. Sci. Rev., 25(1-2), 9-32. https://doi.org/10.1016/j.quascirev.2005.08.008

705   Borges, P. A. V., Santos, A. M. C., Elias, R. B., & Gabriel, R. (2019). The Azores Archipelago:

706   Biodiversity Erosion and Conservation Biogeography. Reference Module in Earth Systems

707   and Environmental Sciences. https://doi.org/10.1016/b978-0-12-409548-9.11949-9

708   Brenner, M., Whitmore, T. J., Curtis, J. H., Hodell, D. A., Schelske, C. L., 1999. Stable isotope

709   (δ^{13}C and δ^{15}N) signatures of sedimented organic matter as indicators of historic lake trophic

710   state. J. Paleolimnol., 22(2), 205-221. https://doi.org/10.1007/s10933-012-9593-6

711   Buckles, L. K., Villanueva, L., Weijers, J. W., Verschuren, D., Damsté, J. S. S., 2013. Linking

712   isoprenoidal GDGT membrane lipid distributions with gene abundances of ammonia-

713   oxidizing Thaumarchaeota and uncultured crenarchaeotal groups in the water column of a

714   tropical lake (Lake Challa, East Africa). Environ. Microbiol., 15(9), 2445-2462.

715   https://doi.org/10.1111/1462-2920.12118

716   Bull, I. D., Lockheart, M. J., Elhmmali, M. M., Roberts, D. J., Evershed, R. P., 2002. The origin

717   of faeces by means of biomarker detection. Environ. Int., 27(8), 647-654.

718   https://doi.org/10.1016/s0160-4120(01)00124-6

719   Calado, H., Borges, P., Phillips, M., Ng, K., Alves, F., 2011. The Azores archipelago, Portugal:

720   improved understanding of small island coastal hazards and mitigation measures. Nat

721   Hazards 58, 427–444. https://doi.org/10.1007/s11069-010-9676-5

722   Castilla-Beltrán, A., de Nascimento, L., Fernández-Palacios, J. M., Fonville, T., Whittaker, R. J.,

723   Edwards, M., Nogué, S., 2019. Late Holocene environmental change and the anthropization

724   of the highlands of Santo Antão Island, Cabo Verde. Palaeogeogr., Palaeoclimatol.,

725   Palaeoecol., 524, 101-117. https://doi.org/10.1016/j.palaeo.2019.03.033

726   Connor, S. E., van Leeuwen, J. F., Rittenour, T. M., van der Knaap, W. O., Ammann, B., Björck,

727   S., 2012. The ecological impact of oceanic island colonization–a palaeoecological

728   perspective from the Azores. J. Biogeogr., 39(6), 1007-1023. https://doi.org/10.1111/j.1365-

729   2699.2011.02671.x

730   Cordeiro, R., Luz, R., Vilaverde, J., Vasconcelos, V., Fonseca, A., Gonçalves, V., 2020.

731   Distribution of Toxic Cyanobacteria in Volcanic Lakes of the Azores Islands. Water, 12(12),

732   3385. https://doi.org/10.3390/w12123385

733   Craig, H., 1961. Isotopic variations in meteoric waters. Science, 133(3465), 1702-1703.

734   https://doi.org/10.1126/science.133.3465.1702

735   Cranwell, P. A., 1973. Chain-length distribution of *n*-alkanes from lake sediments in relation to

736   post-glacial environmental change. Freshw. Biol., 3(3), 259-265.

737   https://doi.org/10.1111/j.1365-2427.1973.tb00921.x

738 Cropper, T. E., Hanna, E., 2014. An analysis of the climate of Macaronesia, 1865–2012. Int. J.

739   Climatol., 34(3), 604-622. https://doi.org/10.1002/joc.3710

740 Crosby, A. W. (2004). *Ecological imperialism: the biological expansion of Europe, 900-1900.*

741   Cambridge University Press.

742 Cruz, J. V., Pacheco, D., Porteiro, J., Cymbron, R., Mendes, S., Malcata, A., Andrade, C., 2015.

743   Sete Cidades and Furnas lake eutrophication (São Miguel, Azores): Analysis of long-term

744   monitoring data and remediation measures. Sci. Total Environ., 520, 168-186.

745   https://doi.org/10.1016/j.scitotenv.2015.03.052

746 Dansgaard, W., 1964. Stable isotopes in precipitation. Tellus, 16(4), 436-468.

747   https://doi.org/10.1111/j.2153-3490.1964.tb00181.x

748 de Nascimento, L., Willis, K. J., Fernández-Palacios, J. M., Criado, C., Whittaker, R. J., 2009.

749   The long-term ecology of the lost forests of La Laguna, Tenerife (Canary Islands). J.

750   Biogeogr., 36(3), 499-514. https://doi.org/10.1111/j.1365-2699.2008.02012.x

751 Dias, E., Mendes, C., Melo, C., Pereira, D., Elias, R., 2005. Azores Central Islands vegetation

752   and flora field guide. Quercetea, 7, 123-173.

753 Dickinson, C. H., & Underhay, V. H. S., 1977. Growth of fungi in cattle dung. Trans. Brit.

754   Mycol. Soc., 69(3), 473-477. https://doi.org/10.1016/S0007-1536(77)80086-7

755 Diefendorf, A. F., Freeman, K. H., Wing, S. L., Graham, H. V., 2011. Production of n-alkyl

756   lipids in living plants and implications for the geologic past. Geochim. Cosmochim. Acta,

757   75(23), 7472-7485. https://doi.org/10.1016/j.gca.2011.09.028

758 Douglas, M. S., Smol, J. P., Savelle, J. M., Blais, J. M., 2004. Prehistoric Inuit whalers affected

759   Arctic freshwater ecosystems. Proc. Nat. Acad. Sci., 101(6), 1613-1617.

760   https://doi.org/10.1073/pnas.0307570100

761   Ekdahl, E. J., Teranes, J. L., Guilderson, T. P., Turton, C. L., McAndrews, J. H., Wittkop, C. A.,

762   Stoermer, E. F., 2004. Prehistorical record of cultural eutrophication from Crawford Lake,

763   Canada. Geology, 32(9), 745-748. https://doi.org/10.1130/G20496.1

764   Esper, J., Frank, D., Büntgen, U., Verstege, A., Luterbacher, J., Xoplaki, E. 2007. Long-term

765   drought severity variations in Morocco. Geophys. Res. Lett., 34(17).

766   https://doi.org/10.1029/2007GL030844

767   Frias, R., 2000. EUROSION Case Study.

768   Gaskell, S. J., Eglinton, G., 1975. Rapid hydrogenation of sterols in a contemporary lacustrine

769   sediment. Nature, 254(5497), 209-211. https://doi.org/10.1038/254209b0

770   Gill, J. L., McLauchlan, K. K., Skibbe, A. M., Goring, S., Zirbel, C. R., Williams, J. W., 2013.

771   Linking abundances of the dung fungus *Sporormiella* to the density of bison: implications for

772   assessing grazing by megaherbivores in palaeorecords. J. Ecol., 101(5), 1125-1136.

773   https://doi.org/10.1111/1365-2745.12130

774   Gimeno L., Nieto R., Trigo R.M., Vicente-Serrano S.M, Lopes-Moreno J.I., 2010. Where does

775   the Iberian Peninsula moisture come from? An answer based on a Lagrangian approach. J.

776   Hydrometeorol., 11, 421-436. https://doi.org/10.1175/2009JHM1182.1

777   *Global Historical Climatology Network (GHCN). NOAA,* https://www.ncdc.noaa.gov/

778   Gordo, C., Zêzere, J. L., Marques, R., 2019. Landslide susceptibility assessment at the basin

779   scale for rainfall-and earthquake-triggered shallow slides. Geosciences, 9(6), 268.

780   https://doi.org/10.3390/geosciences9060268

781   Guillemot, T., Bichet, V., Gauthier, E., Zocatelli, R., Massa, C., Richard, H. 2017.

782   Environmental responses of past and recent agropastoral activities on south Greenlandic

783   ecosystems through molecular biomarkers. Holocene, 27(6), 783-795.

784   https://doi.org/10.1177/0959683616675811

785   Hannon, G. E., Bradshaw, R. H., Bradshaw, E. G., Snowball, I., Wastegård, S., 2005. Climate

786   change and human settlement as drivers of late-Holocene vegetational change in the Faroe

787   Islands. Holocene, 15(5), 639-647. https://doi.org/10.1191/0959683605hl840rp

788   Hernández, A., Kutiel, H., Trigo, R. M., Valente, M. A., Sigró, J., Cropper, T., Santo, F. E.,

789   2016. New Azores Archipelago daily precipitation dataset and its links with large-scale

790   modes of climate variability. Int. J. Climatol., 36(14), 4439-4454.

791   https://doi.org/10.1002/joc.4642

792   Hernández, A., Sáez, A., Bao, R., Raposeiro, P.M., Trigo, R.M., Doolittle, S., Masqué, P., Rull,

793   V., Gonçalves, V., Vázquez-Loureiro, D., Rubio-Inglés, M.J., 2017. The influences of the

794   AMO and NAO on the sedimentary infill in an Azores Archipelago lake since ca. 1350

795   CE. Glob. Planet. Change, 154, 61-74. https://doi.org/10.1016/j.gloplacha.2017.05.007

796   Hillbrand, M., van Geel, B., Hasenfratz, A., Hadorn, P., Haas, J. N., 2014. Non-pollen

797   palynomorphs show human-and livestock-induced eutrophication of Lake Nussbaumersee

798   (Thurgau, Switzerland) since Neolithic times (3840 BC). Holocene, 24(5), 559-568.

799   https://doi.org/10.1177/0959683614522307

800   Hodell, D. A., Schelske, C. L., 1998. Production, sedimentation, and isotopic composition of

801   organic matter in Lake Ontario. Limnol. Oceanogr., 43(2), 200-214.

802   https://doi.org/10.4319/lo.1998.43.2.0200

803   Hoegh-Guldberg, O., D. Jacob, M. Taylor, M. Bindi, S. Brown, I. Camilloni, A. Diedhiou, R.

804   Djalante, K.L. Ebi, F. Engelbrecht, J. Guiot, Y. Hijioka, S. Mehrotra, A. Payne, S.I.

805   Seneviratne, A. Thomas, R. Warren, G. Zhou, 2018: Impacts of 1.5°C Global Warming on

806　　　Natural and Human Systems. In: *Global Warming of 1.5°C. An IPCC Special Report on the*

807　　　*impacts of global warming of 1.5°C above pre-industrial levels and related global*

808　　　*greenhouse gas emission pathways, in the context of strengthening the global response to the*

809　　　*threat of climate change, sustainable development, and efforts to eradicate poverty* [Masson-

810　　　Delmotte, V., P. Zhai, H.-O. P.rtner, D. Roberts, J. Skea, P.R. Shukla, A. Pirani, W.

811　　　Moufouma-Okia, C. P.an, R. Pidcock, S. Connors, J.B.R. Matthews, Y. Chen, X. Zhou, M.I.

812　　　Gomis, E. Lonnoy, T. Maycock, M. Tignor, and T. Waterfield (eds.)].

813　Hollander, D. J., Smith, M. A., 2001. Microbially mediated carbon cycling as a control on the

814　　　$\delta^{13}C$ of sedimentary carbon in eutrophic Lake Mendota (USA): new models for interpreting

815　　　isotopic excursions in the sedimentary record. Geochim. Cosmochim. Acta, 65(23), 4321-

816　　　4337. https://doi.org/10.1016/S0016-7037(00)00506-8

817　Hopmans, E. C., Schouten, S., Damsté, J. S. S., 2016. The effect of improved chromatography on

818　　　GDGT-based palaeoproxies. *Org. Geochem.*, *93*, 1-6.

819　　　https://doi.org/10.1016/j.orggeochem.2015.12.006

820　Huang, W. Y., Meinschein, W. G., 1976. Sterols as source indicators of organic materials in

821　　　sediments. Geochim. Cosmochim. Acta, 40(3), 323-330. https://doi.org/10.1016/0016-

822　　　7037(76)90210-6

823　Huang, W. Y., Meinschein, W. G., 1979. Sterols as ecological indicators. Geochim. Cosmochim.

824　　　Acta, 43(5), 739-745. https://doi.org/10.1016/0016-7037(79)90257-6

825　Huguet, C., Hopmans, E. C., Febo-Ayala, W., Thompson, D. H., Damsté, J. S. S., Schouten, S.,

826　　　2006. An improved method to determine the absolute abundance of glycerol dibiphytanyl

827　　　glycerol tetraether lipids. Org. Geochem., 37(9), 1036-1041.

828　　　https://doi.org/10.1016/j.orggeochem.2006.05.008

829   Hurrell, J. W., 1995. Decadal trends in the North Atlantic Oscillation: regional temperatures and

830   precipitation. Science, 269(5224), 676-679. https://doi.org/10.1126/science.269.5224.676

831   *IAEA/WMO: Global Network of Isotopes in Precipitation. The GNIP Database*,

832   2006, http://www.iaea.org/water.

833   Kalff, J., 2002. *Limnology: inland water ecosystems*. Upper Saddle River, NJ: Prentice-Hall Inc.

834   Kumar, D. M., Woltering, M., Hopmans, E. C., Damsté, J. S. S., Schouten, S., Werne, J. P.,

835   2019. The vertical distribution of Thaumarchaeota in the water column of Lake Malawi

836   inferred from core and intact polar tetraether lipids. Org. Geochem., 132, 37-49.

837   https://doi.org/10.1016/j.orggeochem.2019.03.004

838   Lages, G., 2000. Situação das Flores e do Corvo nos séculos XVI e XVII. Arquipélago - História

839   2, 29–88.

840   Lawson, I.T., Church, M.J., McGovern, T.H., Arge, S.V., Woollet, J., Edwards, K.J., Gathorne-

841   Hardy, F.J., Dugmore, A.J., Cook, G., Mairs, K.A., Thomson, A.M., 2005. Historical ecology

842   on Sandoy, Faroe Islands: palaeoenvironmental and archaeological perspectives. Hum.

843   Ecol., 33(5), 651-684. https://doi.org/10.1007/s10745-005-7681-1

844   Lawson, I. T., Gathorne-Hardy, F. J., Church, M. J., Newton, A. J., Edwards, K. J., Dugmore, A.

845   J., Einarsson, A., 2007. Environmental impacts of the Norse settlement: palaeoenvironmental

846   data from Mývatnssveit, northern Iceland. Boreas, 36(1), 1-19.

847   https://doi.org/10.1111/j.1502-3885.2007.tb01176.x

848   Leeming, R., Ball, A., Ashbolt, N., Nichols, P., 1996. Using faecal sterols from humans and

849   animals to distinguish faecal pollution in receiving waters. Water Res., 30(12), 2893-2900.

850   https://doi.org/10.1016/S0043-1354(96)00011-5

851 Lloyd, C. E., Michaelides, K., Chadwick, D. R., Dungait, J. A., Evershed, R. P., 2012. Tracing

852   the flow-driven vertical transport of livestock-derived organic matter through soil using

853   biomarkers. Org. Geochem., 43, 56-66. https://doi.org/10.1016/j.orggeochem.2011.11.001

854 Maffei, M., 1996. Chemotaxonomic significance of leaf wax alkanes in the

855   Gramineae. Biochem. Syst. Ecol., 24(1), 53-64. https://doi.org/10.1016/0305-

856   1978(95)00102-6

857 Marques R., Zezere J.L., Trigo R.M., Gaspar J.L., Trigo I.F., 2008. Rainfall patterns and critical

858   values associated with landslides in Povoação County (São Miguel Island, Azores):

859   relationships with the North Atlantic Oscillation. Hydrol. Process., 22, 478-494, DOI:

860   10.1002/hyp.6879.

861 Marsden, M. W., 1989. Lake restoration by reducing external phosphorus loading: the influence

862   of sediment phosphorus release. Freshw. Biol., 21(2), 139-162.

863   https://doi.org/10.1111/j.1365-2427.1989.tb01355.x

864 Massa, C., Bichet, V., Gauthier, É., Perren, B.B., Mathieu, O., Petit, C., Monna, F., Giraudeau,

865   J., Losno, R., Richard, H., 2012. A 2500 year record of natural and anthropogenic soil

866   erosion in South Greenland. Quat. Sci. Rev., 32, 119-130.

867   https://doi.org/10.1016/j.quascirev.2011.11.014

868 Meneses, A. de F. de, 2009. Os Açores e os Impérios - séculos XV a XX. Arquipélago - História

869   XIII, 205–218.

870 Meyers, P. A., 2003. Applications of organic geochemistry to paleolimnological reconstructions:

871   a summary of examples from the Laurentian Great Lakes. Org. Geochem., 34(2), 261-289.

872   https://doi.org/10.1016/S0146-6380(02)00168-7

873 Mortlock, R. A., Froelich, P. N., 1989. A simple method for the rapid determination of biogenic

874   opal in pelagic marine sediments. Deep Sea Res. Part A. Oceanogr. Res. Pap., 36(9), 1415-

875   1426. https://doi.org/10.1016/0198-0149(89)90092-7

876 Muggeo, V.M., 2008. segmented: an R Package to Fit Regression Models with Broken-Line

877   Relationships. *R News*, 8(1), 20–25. https://cran.r-project.org/doc/Rnews/.

878 Naeher, S., Peterse, F., Smittenberg, R. H., Niemann, H., Zigah, P. K., Schubert, C. J., 2014.

879   Sources of glycerol dialkyl glycerol tetraethers (GDGTs) in catchment soils, water column

880   and sediments of Lake Rotsee (Switzerland)–Implications for the application of GDGT-based

881   proxies for lakes. Org. Geochem., 66, 164-173.

882   https://doi.org/10.1016/j.orggeochem.2013.10.017

883 Nishimura, M., Koyama, T., 1977. The occurrence of stanols in various living organisms and the

884   behavior of sterols in contemporary sediments. Geochim. Cosmochim. Acta, 41(3), 379-385.

885   https://doi.org/10.1016/0016-7037(77)90265-4

886 Nishimura, M., 1977. Origin of stanols in young lacustrine sediments. Nature, 270(5639), 711-

887   712. https://doi.org/10.1038/270711a0

888 Pancost, R.D., van Geel, B., Baas, M., Sinninghe Damsté, J.S., 2000. δ^{13}C values and

889   radiocarbon dates of microbial biomarkers as tracers for carbon recycling in peat deposits.

890   Geology, 28, 663–666. https://doi.org/10.1130/0091-

891   7613(2000)28<663:CVARDO>2.0.CO;2

892 Pancost, R.D., Hopmans, E.C., Sinninghe Damsté, J.S., 2001. Archaeal lipids in Mediterranean

893   cold seeps: molecular proxies for anaerobic methane oxidation. Geochim. Cosmochim. Acta,

894   65, 1611–1627. https://doi.org/10.1016/S0016-7037(00)00562-7

895   Pearson, A., Huang, Z., Ingalls, A.E., Romanek, C.S., Wiegel, J., Freeman, K.H., Smittenberg,

896   R.H., Zhang, C.L., 2004. Nonmarine crenarchaeol in Nevada hot springs. Appl. Environ.

897   Microbiol., 70(9), 5229-5237. https://doi.org/10.1128/AEM.70.9.5229-5237.2004

898   Perrotti, A.G., van Asperen, E., 2019. Dung fungi as a proxy for megaherbivores: opportunities

899   and limitations for archaeological applications. Veget. Hist. Archaeobot. 28, 93–104.

900   https://doi.org/10.1007/s00334-018-0686-7

901   Pitcher, A., Rychlik, N., Hopmans, E.C., Spieck, E., Rijpstra, W.I.C., Ossebaar, J., Schouten, S.,

902   Wagner, M., Sinninghe Damsté, J.S.S., 2010. Crenarchaeol dominates the membrane lipids

903   of *Candidatus Nitrososphaera gargensis*, a thermophilic Group I. 1b Archaeon. ISME

904   J., 4(4), 542-552. https://doi.org/10.1038/ismej.2009.138

905   Pitcher, A., Hopmans, E.C., Mosier, A.C., Park, S.J., Rhee, S.K., Francis, C.A., Schouten, S.,

906   Sinninghe Damsté, J.S., 2011. Core and intact polar glycerol dibiphytanyl glycerol tetraether

907   lipids of ammonia-oxidizing archaea enriched from marine and estuarine sediments. Appl.

908   Environ. Microbiol., 77(10), 3468-3477. https://doi.org/10.1128/AEM.02758-10

909   Pouliot, J., Galand, P. E., Lovejoy, C., Vincent, W. F., 2009. Vertical structure of archaeal

910   communities and the distribution of ammonia monooxygenase A gene variants in two

911   meromictic High Arctic lakes. Environ. Microbiol., 11(3), 687-699.

912   https://doi.org/10.1111/j.1462-2920.2008.01846.x

913   Raposeiro, P.M., Hernández, A., Pla-Rabes, S., Bao, R. Sáez, A., Benavente, M. Richter, N., de

914   Groff, W., de Boer, E.J., Ritter, C. Amaral-Zettler, L.A., Giralt, S. 2021a. Multi-proxy

915   analysis of sediment cores from Lake Funda (Azores Archipelago, Portugal). PANGAEA,

916   https://doi.org/10.1594/PANGAEA.933712

917 Raposeiro, P.M., Hernández, A., Pla-Rabes, S., Gonçalves, V., Bao, R., Sáez, A., Shanahan, T.,

918 Benavente, M., de Boer, E., Richter, N., Gordon, V., Marques, H., Sousa, P.M., Souto, M.,

919 Matias, M.G., Aguiar, N., Pereira, C., Ritter, C., Rubio, M.J., Salcedo, M., Vázquez-

920 Loureiro, D., Margalef, O., Amaral-Zettler, L.A., Costa, A.C., Huang, Y., van Leeuwen,

921 J.F.N., Masqué, P., Prego, R., Ruiz-Fernández, A.C., Sánchez-Cabeza, J., Trigo, R., Giralt,

922 S., 2021b. Climate change facilitated the early colonization of the Azores Archipelago during

923 Medieval times. Proc. Natl. Acad. Sci., 118(41), e2108236118.

924 https://doi.org/10.1073/pnas.2108236118

925 Raposeiro, P.M., Rubio, M.J., González, A., Hernández, A., Sánchez-López, G., Vázquez-

926 Loureiro, D., Rull, V., Bao, R., Costa, A.C., Gonçalves, V., Sáez, A., 2017. Impact of the

927 historical introduction of exotic fishes on the chironomid community of Lake Azul (Azores

928 Islands). Palaeogeogr., Palaeoclimatol., Palaeoecol., 466, 77-88.

929 https://doi.org/10.1016/j.palaeo.2016.11.015

930 Reimer, P.J., Bard, E., Bayliss, A., Beck, J.W., Blackwell, P.G., Ramsey, C.B., Buck, C.E.,

931 Cheng, H., Edwards, R.L., Friedrich, M., Grootes, P.M., Guilderson, T.P., Haflidason, H.,

932 Hajdas, I., Hatté, C., Heaton, T.J., Hoffmann, D.L., Hogg, A.G., Hughen, K.A., Kaiser, K.F.,

933 Kromer, B., Manning, S.W., Niu, M., Reimer, R.W., Richards, D.A., Scott, E.M., Southon,

934 J.R., Staff, R.A., Turney, C.S.M., van der Plicht, J., 2013. IntCal13 and Marine13

935 radiocarbon age calibration curves 0–50,000 years cal BP. Radiocarbon, 55, 1869–1887.

936 https://doi.org/10.2458/azu_js_rc.55.16947

937 Richter, N., Russell, J.M., Garfinkel, J., Huang, Y., 2021. Impacts of Norse settlement on

938 terrestrial and aquatic ecosystems in Southwest Iceland. J. Paleolimnol., 65(2), 255-269.

939 https://doi.org/10.1007/s10933-020-00169-3

940 Richter, N., Russell, J. M., Amaral-Zettler, L. A., DeGroff, W., Raposeiro, P.M., Gonçalves, V.,

941   Pla-Rabes, S., Hernández, A., Benavente, M., Ritter, C., Bao, R., Prego, R., Giralt, S., 2022.

942   Organic geochemical analysis of sediment cores from Lake Funda (Azores Archipelago,

943   Portugal). PANGAEA, https://doi.org/10.1594/PANGAEA.941316

944 Ritter, C., Gonçalves, V., Pla-Rabes, S., de Boer, E.J., Bao, R., Sáez, A., Hernández, A., Sixto,

945   M., Richter, N., Benavente, M., Prego, R., Giralt, S., Raposeiro, P.M., 2022. The vanishing

946   and the establishment of a new ecosystem on an oceanic island – Anthropogenic impacts

947   with no return ticket. Sci. Total Environ. 154828.

948   https://doi.org/https://doi.org/10.1016/j.scitotenv.2022.154828

949 Rubio de Inglés, M. J., 2016. Late Holocene Climate Variability in the North Atlantic based on

950   biomarker reconstruction: The lake Azul (São Miguel, Azores Archipelago) case.

951 Rull, V., Lara, A., Rubio-Inglés, M.J., Giralt, S., Gonçalves, V., Raposeiro, P., Hernández, A.,

952   Sánchez-López, G., Vázquez-Loureiro, D., Bao, R., Masqué, P., 2017. Vegetation and

953   landscape dynamics under natural and anthropogenic forcing on the Azores Islands: A 700-

954   year pollen record from the São Miguel Island. Quat. Sci. Rev., 159, 155-168.

955   https://doi.org/10.1016/j.quascirev.2017.01.021

956 Sachse, D., Billault, I., Bowen, G.J., Chikaraishi, Y., Dawson, T.E., Feakins, S.J., Freeman,

957   K.H., Magill, C.R., McInerney, F.A., Van Der Meer, M.T., Polissar, P., 2012. Molecular

958   paleohydrology: interpreting the hydrogen-isotopic composition of lipid biomarkers from

959   photosynthesizing organisms. Annu. Rev. Earth Planet. Sci., 40, 221-249.

960   https://doi.org/10.1146/annurev-earth-042711-105535

961 Sánchez-López, G., Hernández, A., Pla-Rabès, S., Trigo, R.M., Toro, M., Granados, I., Sáez, A.,

962   Masqué, P., Pueyo, J.J., Rubio-Inglés, M.J., Giralt, S., 2016. Climate reconstruction for the

963   last two millennia in central Iberia: The role of East Atlantic (EA), North Atlantic Oscillation

964   (NAO) and their interplay over the Iberian Peninsula. Quat. Sci. Rev., 149, 135-150.

965   https://doi.org/10.1016/j.quascirev.2016.07.021

966   Santos, F. D., Valente, M. A., Miranda, P. M. A., Aguiar, A., Azevedo, E. B., Tomé, A. R.,

967   Coelho, F., 2004. Climate change scenarios in the Azores and Madeira Islands. World

968   Resour. Rev., 16(4), 473-491.

969   Schäfer, H., 2003. Chorology and diversity of the Azorean flora. Willdenowia, 33, 481-482.

970   Scheffer, M., 1998. Ecology of shallow lakes (Vol. 1). London: Chapman & Hall.

971   Scheffer, M., Carpenter, S., Foley, J. A., Folke, C., Walker, B., 2001. Catastrophic shifts in

972   ecosystems. Nature, 413(6856), 591-596. https://doi.org/10.1038/35098000

973   Schindler, D. W., 2006. Recent advances in the understanding and management of

974   eutrophication. Limnol. Oceanogr., 51, 356-363.

975   https://doi.org/10.4319/lo.2006.51.1_part_2.0356

976   Schouten, S., Hopmans, E.C., Baas, M., Boumann, H., Standfest, S., Könneke, M., Stahl, D.A.,

977   Sinninghe Damsté, J.S., 2008. Intact membrane lipids of "*Candidatus Nitrosopumilus*

978   *maritimus*," a cultivated representative of the cosmopolitan mesophilic group I

979   Crenarchaeota. Appl. Environ. Microbiol., 74(8), 2433-2440.

980   https://doi.org/10.1128/AEM.01709-07

981   Schouten, S., Hopmans, E. C., Damsté, J. S. S., 2013. The organic geochemistry of glycerol

982   dialkyl glycerol tetraether lipids: a review. Org. Geochem., 54, 19-61.

983   https://doi.org/10.1016/j.orggeochem.2012.09.006

984   Schwark, L., Zink, K., Lechterbeck, J., 2002. Reconstruction of postglacial to early Holocene

985   vegetation history in terrestrial Central Europe via cuticular lipid biomarkers and pollen

986 records from lake sediments. Geology, 30(5), 463-466. https://doi.org/10.1130/0091-

987 7613(2002)030<0463:ROPTEH>2.0.CO;2

988 Sinninghe Damsté, J. S., Schouten, S., Hopmans, E. C., Van Duin, A. C., Geenevasen, J. A.,

989 2002. Crenarchaeol. J. Lipid Res., 43(10), 1641-1651. https://doi.org/10.1194/jlr.M200148-

990 JLR200

991 Sinninghe Damsté, J. S., Ossebaar, J., Abbas, B., Schouten, S., Verschuren, D., 2009. Fluxes and

992 distribution of tetraether lipids in an equatorial African lake: constraints on the application of

993 the TEX_{86} palaeothermometer and BIT index in lacustrine settings. Geochim. Cosmochim.

994 Acta, 73(14), 4232-4249. https://doi.org/10.1016/j.gca.2009.04.022

995 Sinninghe Damsté, J.S., Rijpstra, W.I.C., Hopmans, E.C., Jung, M.Y., Kim, J.G., Rhee, S.K.,

996 Stieglmeier, M., Schleper, C., 2012. Intact polar and core glycerol dibiphytanyl glycerol

997 tetraether lipids of group I. 1a and I. 1b Thaumarchaeota in soil. App. Environ.

998 Microbiol., 78(19), 6866-6874. https://doi.org/10.1128/AEM.01681-12

999 Skov, T., Buchaca, T., Amsinck, S.L., Landkildehus, F., Odgaard, B.V., Azevedo, J., Gonçalves,

1000 V., Raposeiro, P.M., Andersen, T.J., Jeppesen, E., 2010. Using invertebrate remains and

1001 pigments in the sediment to infer changes in trophic structure after fish introduction in Lake

1002 Fogo: a crater lake in the Azores. Hydrobiologia, 654(1), 13-25.

1003 https://doi.org/10.1007/s10750-010-0325-5

1004 Smith, S. H., 2010. The mid-Atlantic islands: A theatre of early modern ecocide?. Int. Rev. Soc.

1005 Hist., 55(S18), 51-77.

1006 Tipple, B. J., Berke, M. A., Doman, C. E., Khachaturyan, S., Ehleringer, J. R. 2013. Leaf-wax n-

1007 alkanes record the plant–water environment at leaf flush. Proc. Nat. Acad. Sci., 110(7), 2659-

1008 2664. https://doi.org/10.1073/pnas.1213875110

1009   van Bree, L.G.J., Peterse, F., Van der Meer, M.T.J., Middelburg, J.J., Negash, A.M.D., De Crop,

1010   W., Cocquyt, C., Wieringa, J.J., Verschuren, D., Damsté, J.S., 2018. Seasonal variability in

1011   the abundance and stable carbon-isotopic composition of lipid biomarkers in suspended

1012   particulate matter from a stratified equatorial lake (Lake Chala, Kenya/Tanzania):

1013   Implications for the sedimentary record. Quat. Sci. Rev., 192, 208-224.

1014   https://doi.org/10.1016/j.quascirev.2018.05.023

1015   Vázquez-Loureiro, D., Gonçalves, V., Sáez, A., Hernández, A., Raposeiro, P.M., Giralt, S.,

1016   Rubio-Inglés, M.J., Rull, V. and Bao, R., 2019. Diatom-inferred ecological responses of an

1017   oceanic lake system to volcanism and anthropogenic perturbations since 1290 CE.

1018   Palaeogeogr., Palaeoclimatol., Palaeoecol., 534, p.109285.

1019   https://doi.org/10.1016/j.palaeo.2019.109285

1020   Volkman, J. K., 1986. A review of sterol markers for marine and terrigenous organic matter.

1021   Org. Geochem., 9(2), 83-99. https://doi.org/10.1016/0146-6380(86)90089-6

1022   Wakeham, S. G., Lewis, C. M., Hopmans, E. C., Schouten, S., Sinninghe Damsté, J. S., 2003.

1023   Archaea mediate anaerobic oxidation of methane in deep euxinic waters of the Black

1024   Sea. Geochim. Cosmochim. Acta, 67(7), 1359-1374. https://doi.org/10.1016/S0016-

1025   7037(02)01220-6

1026   Walker, R. W., Wun, C. K., Litsky, W., & Dutka, B. J., 1982. Coprostanol as an indicator of

1027   fecal pollution. Crit. Rev. Environ. Sci. Technol., 12(2), 91-112.

1028   https://doi.org/10.1080/10643388209381695

1029   Wassenburg, J.A., Immenhauser, A., Richter, D.K., Niedermayr, A., Riechelmann, S., Fietzke,

1030   J., Scholz, D., Jochum, K.P., Fohlmeister, J., Schröder-Ritzrau, A., Sabaoui, A., 2013.

1031   Moroccan speleothem and tree ring records suggest a variable positive state of the North

1032   Atlantic Oscillation during the Medieval Warm Period. Earth Planet. Sci. Lett., 375, 291-302.

1033   https://doi.org/10.1016/j.epsl.2013.05.048

1034 Wood, J. R., Wilmshurst, J. M., 2012. Wetland soil moisture complicates the use of *Sporormiella*

1035   to trace past herbivore populations. J. Quat. Sci., 27(3), 254-259.

1036   https://doi.org/10.1002/jqs.1539

1037 Woolway, R.I., Merchant, C.J., 2019. Worldwide alteration of lake mixing regimes in response

1038   to climate change. Nat. Geosci. 12, 271–276. https://doi.org/10.1038/s41561-019-0322-x

1039 Zocatelli, R., Lavrieux, M., Guillemot, T., Chassiot, L., Le Milbeau, C., Jacob, J. 2017. Fecal

1040   biomarker imprints as indicators of past human land uses: Source distinction and preservation

1041   potential in archaeological and natural archives. J. Archaeol. Sci., 81, 79-89.

1042   https://doi.org/10.1016/j.jas.2017.03.010